



HAL
open science

The Theoretical Shapley-Shubik Probability of an Election Inversion in a Toy Symmetric Version of the U.S. Presidential Electoral System

Olivier de Mouzon, Thibault Laurent, Michel Le Breton, Dominique Lepelley

► **To cite this version:**

Olivier de Mouzon, Thibault Laurent, Michel Le Breton, Dominique Lepelley. The Theoretical Shapley-Shubik Probability of an Election Inversion in a Toy Symmetric Version of the U.S. Presidential Electoral System. *Social Choice and Welfare*, 2020, 54 (2-3), pp.363-395. 10.1007/s00355-018-1162-0 . hal-02547744

HAL Id: hal-02547744

<https://hal.science/hal-02547744>

Submitted on 20 Apr 2020

HAL is a multi-disciplinary open access archive for the deposit and dissemination of scientific research documents, whether they are published or not. The documents may come from teaching and research institutions in France or abroad, or from public or private research centers.

L'archive ouverte pluridisciplinaire **HAL**, est destinée au dépôt et à la diffusion de documents scientifiques de niveau recherche, publiés ou non, émanant des établissements d'enseignement et de recherche français ou étrangers, des laboratoires publics ou privés.

The Theoretical Shapley-Shubik Probability of an Election Inversion in a Toy Symmetric Version of the U.S. Presidential Electoral System*

Olivier de Mouzon[†] Thibault Laurent[‡] Michel Le Breton[§]
Dominique Lepelley[¶]

February 2018

Abstract

In this article, we evaluate asymptotically the probability $\phi(n)$ of an election inversion in a toy symmetric version of the U.S. presidential electoral system. The novelty of this paper, in contrast to all the existing theoretical literature, is to assume that votes are drawn from an IAC (Impartial Anonymous Culture)/Shapley-Shubik probability model. Through the use of numerical methods, it is conjectured that $\sqrt{n}\phi(n)$ converges to a limit when n (the size of the electorate in one district)

*We thank the guest editor, Kotaro Suzumura and the referee for their encouragements as well as all the participants of the 13th Social Choice and Welfare conference (Lund, 2016), as well as the participants of the 13th meeting of the “Ingénieurs Statisticiens Toulousains” (Toulouse, July 2015), for their comments and suggestions. We would like to express our deepest gratitude to Kazuya Kikuchi, Vincent Merlin and Isofa Moyouwou for the very insightful comments and suggestions contained in the scientific correspondence that we had with them on the topic covered by this paper. Out of that, Kikuchi (2018) provides a short, elegant and assumption-free proof of the convergence to 0 of the IAC probability of an election inversion when the number of voters tends to infinity. Of course, any remaining errors are ours. For replication, the codes are available at: <http://www.thibault.laurent.free.fr/code/IAC/>. The codes are also described in appendix D. Michel Le Breton and Dominique Lepelley would like to express their immense respect and gratitude to Ken Arrow to whom this special issue is dedicated. Ken Arrow was interested in many topics (not to say all) and majority voting (the topic of the current paper) was among them. The first (1951) edition contains discussions of majority voting and more generally of the application of his theory to elections. For instance, on page 6, he writes “...The chief relevant point here is that virtually every particular scheme proposed for election from single-member constituencies has been shown to have certain arbitrary features. *The problem of choosing one among a number of candidates for a single position, such as the Presidency of the United States...* is clearly of the same character as choosing one out of a number of alternative social policies”. The addition that appears in the second (1963) edition contains historical remarks including a discussion of the contribution of Condorcet to the theory of voting. The French translation appears in 1974. It contains a foreword, dated August 10, 1974, intended for the French readers. It reminds, among other things, the important work of the French precursors on voting methods and it is concluded as follows: “*J’espère que cette traduction invitera quelques universitaires français à choisir ce domaine de recherche; les spécialistes ont besoin d’eux*”. We accepted that invitation and never regretted, during our all professional life, to have done so.

[†]Toulouse School of Economics, INRA, University of Toulouse Capitole, Toulouse, France.

[‡]Toulouse School of Economics, CNRS, University of Toulouse Capitole, Toulouse, France.

[§]Institut Universitaire de France and Toulouse School of Economics, University of Toulouse Capitole, France.

[¶]CEMOI, Faculté de Droit et de Sciences Économiques et Politiques, Université de La Réunion, France.

tends to infinity. It is also demonstrated that $\text{LimSup}_{\frac{\sqrt{n}}{m(n)^{1.5}}} \phi(n)$ and $\text{LimInf}_{\sqrt{n}} \phi(n)$ are finite numbers.

Classification JEL: D71, D72.

Key Words: Electoral system, Election Inversions, Impartial Anonymous Culture

1 Introduction

As described by Miller (2012a): “An election inversion occurs when the candidate (or party) that wins the most votes from the nationwide electorate fails to win the most electoral votes (or parliamentary seats) and therefore loses the election”. To describe this phenomenon, public commentary commonly uses such terms as ‘reversal of winner’, ‘unpopular winner’, ‘divided verdict’ while the academic literature on voting and social choice uses such terms as ‘compound majority paradox’ and ‘referendum paradox’¹. Election inversions can occur under U.S. Electoral College² or any two-tier electoral system.

The President of the United States is elected, not by a direct national popular vote, but by an indirect Electoral College system in which (in almost universal practice since the 1830s) separate state popular votes are aggregated by adding up state electoral votes awarded, on a winner-take-all basis, to the plurality winner in each state. Each state has electoral votes equal in number to its total representation in Congress and since 1964 the District of Columbia has three electoral votes. Therefore the U.S. Electoral College is a two-tier electoral system: individual voters cast votes in the first tier to choose between rival slates of ‘Presidential electors’ pledged to one or other Presidential candidate, and the winning elector slates then cast blocs of electoral votes for the candidate to whom they are pledged in the second tier. At the present time, there are 538 electoral votes, so 270 are required for election and a 269-269 electoral vote tie is possible. As is well-known, the Electoral College has produced a ‘wrong winner’ in several elections including the 2000 and the 2016 presidential election, and it has done so three times before.

The pervasiveness of the ‘Election Inversions paradox’ raises the following question. Given a division of the country into a number of (possibly unequal) districts, a number of electoral seats for each of those districts and a probability distribution of the Left/Right preferences among the voters, what is the probability that this event will occur? We can approach this question in at least two different ways. A first one, purely theoretical, consists in considering an abstract probability distribution on the set of preference profiles. A second one more empirical consists in estimating the probability distribution on the basis of a statistical model and the electoral data. This paper is a contribution to the first avenue of research.

The literature dedicated to the theoretical probabilistic evaluation of social choice events and paradoxes is dominated by two popular models known under the acronyms *IC* (*Impartial Culture*) and *IAC* (*Impartial Anonymous Culture*). Both models, as well as their extensions, are defined by a specific probability distribution over the set of profiles of voter’s orderings over a finite set of alter-

¹See Nurmi (1999).

²Miller (2012b) contains an insightful presentation of the Electoral College that he qualifies as “a terrific boon for political science (and public choice) research (and teaching)”.

natives/candidates. The *IC* model postulates that the preferences of the voters are independent and identically distributed, the common marginal distribution being the uniform multinomial distribution over the set of feasible orderings³. Equivalently, *IC* postulates that all profiles are equally likely. In contrast, the *IAC* model, introduced for the first time by Fishburn and Gehrlein (1976) and Kuga and Nagatani (1974) postulates that all the situations (a situation is a dispatching of the total population of voters between the different possible preferences) are equally likely. It can be shown that *IAC* is equivalent to the assumption that the preferences of the voters are independent and identically distributed according to a multinomial distribution conditional on a prior uniform⁴ draw of the vector of parameters in the unit simplex whose dimension is the number of feasible orderings. This implies that, while the marginal probabilities are still identical across voters and uniform, voter's preferences are not independent anymore: their preferences exhibit some positive correlation often qualified as describing some homogeneity in the society (Gehrlein and Lepelley (2011))⁵. In this paper, we focus on the case where there are two alternatives and therefore two possible preferences. In such case, the *IC* model is also known as the Banzhaf's model (1965, 1966) and the *IAC* model is known as the Shapley-Shubik's model⁶. The probabilistic connection was pointed out by Straffin (1978). When the population of voters is exogenously partitioned into districts/states/regions, we may consider to combine *IC* and *IAC* in many different ways. In this paper, we denote by *IAC** the probability model according to which the preferences of the voters proceed from *IAC* within districts and are independent across districts. This model was introduced for the first time (without name) by May (1948). Since then, it has been rediscovered by several authors including Chamberlain and Rothschild (1981), Feix, Lepelley, Merlin and Rouet (2004), Good and Mayer (1975) and Le Breton and Lepelley (2014). Le Breton, Lepelley and Smaoui (2016) contains a complete analysis of pivotality of popular majority voting in the context of this model.

To the best of our knowledge, the first theoretical work on election inversions was by May (1948), who calculated the theoretical frequency of election inversions in the case of *IAC**. May limits his investigation to the case of an odd number of equipopulated districts (also with an odd number of voters per district) and one seat per district. He proves among other things that, in such case, the probability of election inversions increases slowly with the number of districts and the number of voters per district and tends to the limit $\frac{1}{6} \simeq 16.7\%$. Feix, Lepelley, Merlin and Rouet (2004) and Lepelley, Merlin and Rouet (2011) also consider the setting of equipopulated districts but do not limit

³If there are m feasible orderings, this means that each marginal distribution is a *multinomial* probability distribution with vector of parameters $(\frac{1}{m}, \frac{1}{m}, \dots, \frac{1}{m})$.

⁴This prior is a special case of a *Dirichlet distribution*.

⁵See Straffin (1988) for a very nice united presentation of *IC* and *IAC*.

⁶In the two-alternative case, the *IC* and *IAC* model have been extensively used to study the fairness of voting bodies from the point of view of the power defined as the expected propensity for a voter to be influent/pivotal in the decision making process. The computation of the Banzhaf and Shapley-Shubik power indices is one of the main area of applied research.

their investigation to the odd case. They have rediscovered some of May's results and have also proceeded to an evaluation of the frequency under *IC*. In the *IC* model, they compute the asymptotic (with respect to the number of voters per district) exact probability for the case of 3, 4 and 5 districts and show through simulations that the asymptotic probability of election inversions increases with the number of districts and tend to 20.5% when the number of districts tend to infinity. This question is already addressed by Hinich, Mickelsen and Ordeshook (1975) who consider a model with equipopulated districts but instead of probabilities on the individual votes, they consider probabilities on the proportions of left voters in each district. The probability distribution of the proportion in each district is assumed to be in the beta family and the proportions are independent across districts; therefore, their model is (in some sense) a generalization of both *IAC** and *IC*. They obtain many interesting results. In particular, in the unbiased case, they show that the probability of election inversions tends to $\frac{\arccos 2(2\pi)^{-\frac{1}{2}}}{\pi} \simeq 20.595\%$ when the number of districts and the beta parameter tend to infinity⁷.

The main objective of this paper is to fill a gap in the theoretical approach⁸. Indeed, while *IAC* is considered as being one of the two most popular probability models in social choice and power measurement, to the best of our knowledge, the evaluation of the probability of election inversions in that case has not been performed so far. The unique contribution to the analysis of the Electoral College considering the *IAC* Shapley-Shubik model is Owen (1975)⁹. As already pointed out, the main difference between *IAC* and *IAC** is the introduction of vote correlations across districts in addition to the vote correlations within districts. Intuitively increasing the positive covariance increases the homogeneity of the electorate and decreases the likelihood of an election inversion. If the correlation was perfect, then the problem of a divided verdict will disappear irrespective of the number of voters. The main contribution of this paper is twofold. First, in section 3, we provide a numerical approach to the evaluation of this probability in the case of three equipopulated districts¹⁰ and *IAC* and show that when n , the number of voters per district, tends to infinity, this probability behaves as $\frac{0.1309}{\sqrt{n}}$. Second, since we have not been able to prove that this is indeed the limit, we provide in section 4

⁷Saying that the beta parameter of the distribution tends to $+\infty$ amounts to say that the probability that the election is tied in any given district tends to 1, which is what postulates the *IC* model.

⁸While this paper is about election inversions, the same apparatus could be used to estimate the votes/seats relationship (see e.g. Tufté (1973)) and the likelihood of any event like 'The left won $x\%$ of the popular vote and $y\%$ of the seats/electoral votes' where both x and y are numbers in $[0, 1]$. If you divide the unit square $[0, 1]^2$ into the four squares $[0, \frac{1}{2}] \times [0, \frac{1}{2}]$, $[0, \frac{1}{2}] \times [\frac{1}{2}, 1]$, $[\frac{1}{2}, 1] \times [0, \frac{1}{2}]$ and $[\frac{1}{2}, 1] \times [\frac{1}{2}, 1]$, the probability of election inversions is the probability of the union of the two anti-diagonal squares. Obviously, knowing the totality of the joint distribution on $[0, 1]^2$ has some intrinsic value that is discussed in the working paper version.

⁹Owen computes the Shapley-Shubik and the Banzhaf powers of the U.S. citizens as a function of the state where they vote. He shows, surprisingly, that the relative powers of the citizen of any state (the denominator is the power of a citizen from the District of Columbia) are about the same for the two models.

¹⁰Most authors in the theoretical vein have considered this toy symmetric version of the Electoral College. Recent developments aiming to an evaluation of the probability of an election inversion in the general case are Kikuchi (2017) and Kaniovski and Zaigraev (2017).

theoretical lower and upper bounds of that probability, which are consistent with this conjecture: The lower bound behaves as $O\left(\frac{1}{\sqrt{n}}\right)$ and the upper bound behaves as $O\left(\frac{\ln(n)^3}{\sqrt{n}}\right)$ ¹¹.

The plan of this paper is as follows. In section 2, we present the problem of a divided verdict in the simplest conceivable setting and the main notations used in the paper, a brief state of the art and a statement of the precise problem studied in this manuscript. Then, in section 3 we develop a numerical approach of that problem and discuss the behavior of these estimations together with two bounds as the number of voters gets very large. Finally, in section 4, we complement the numerical study by two analytic results which reinforce the numerical discoveries upon the speed of convergence. We conclude by formulating some opening questions and avenues of research.

2 The Toy Model: Notations and State of the Art

2.1 Notations and Assumptions

In this paper we explore the simplest non trivial two-tier system. A territory (for instance a country) is divided into three equipopulated¹² districts. Each district elects one representative. We can either see the outcome of these elections as describing the election of the representatives of a parliament or as describing a toy symmetric version of the US electoral college where these three representatives elect the head of the executive of the country. We denote by n the number of voters in each district; n is assumed to be odd. Then, the total number of voters is $3n$. In each election, the voter can chose among two candidates: a left candidate L and a right candidate R. A profile of preferences is a vector X in $\{L, R\}^{3n}$: X_i denotes the preference of voter i .

Ex ante uncertainty is described here by a probability model λ : $\lambda(X)$ denotes the probability of the event X . The three probability models informally described in the introduction are the more popular. They are precisely defined as follows. A more pedestrian and illustrative exposition of these probability models emphasizing their differences in terms of correlation between votes is presented in appendix C.

IC (Impartial Culture): $\lambda(X) = \frac{1}{2^{3n}}$ for all $X \in \{L, R\}^{3n}$. According to *IC*, voters vote independently of each other with an equal probability of voting left or right. The probability of the event ‘ k voters vote left’ is then equal to $\binom{3n}{k} \frac{1}{2^{3n}}$.

IAC (Impartial Anonymous Culture). The probability λ is now defined as follows. We first draw uniformly the parameter p in the interval $[0, 1]$. Then, conditional on the draw of p , the variables X_i are independent and identically distributed according to the Bernoulli law of parameter p . Therefore,

¹¹An immediate corollary of these results is that the probability of an election inversion tends to 0 when the number of voters per district tends to ∞ . Kikuchi (2018) proves that this convergence to 0 holds true for any number of districts and any profile of populations and electoral votes across districts.

¹²So malapportionment is excluded from the scope of our analysis.

if the vector X has k coordinates X_i such that $X_i = L$ (and therefore $n - k$ coordinates X_i such that $X_i = R$), $\lambda(X) = \int_0^1 p^k (1 - p)^{3n - k} dp$. From the standard equality defining the Beta distribution:

$$\int_0^1 x^{\alpha-1} (1-x)^{\beta-1} dx = \frac{\Gamma(\alpha)\Gamma(\beta)}{\Gamma(\alpha+\beta)}, \quad (1)$$

where α and β are positive parameters and Γ is the gamma function¹³, we deduce: $\lambda(X) = \frac{k!(3n-k)!}{(3n+1)!}$. The probability of the event that k voters vote left is now equal to $\binom{3n}{k} \frac{k!(3n-k)!}{(3n+1)!} = \frac{1}{3n+1}$.

*IAC** (District Based Impartial Anonymous Culture). We first draw uniformly and independently in the interval $[0, 1]$ three parameters p_1, p_2 and p_3 . Then, conditional on the draw of (p_1, p_2, p_3) , the variables X_i are independent and identically distributed according to the Bernoulli law of parameter p_j in each district $j = 1, 2, 3$. Therefore, if the vector X has k_j coordinates X_i such that $X_i = L$ (and $n - k_j$ coordinates X_i such that $X_i = R$) in district $j = 1, 2, 3$,

$$\lambda(X) = \left[\int_0^1 p^{k_1} (1-p)^{n-k_1} dp \right] \left[\int_0^1 p^{k_2} (1-p)^{n-k_2} dp \right] \left[\int_0^1 p^{k_3} (1-p)^{n-k_3} dp \right].$$

From (1), we deduce:

$$\lambda(X) = \frac{k_1!(n-k_1)!}{(n+1)!k_1!(n-k_1)!} \frac{k_2!(n-k_2)!}{(n+1)!} \frac{k_3!(n-k_3)!}{(n+1)!}$$

The computation of the probability of the event that k voters vote left is more subtle. In contrast, the probability of the event that k_1 voters of district 1 vote left, k_2 voters of district 2 vote left and k_3 voters of district 3 vote left is equal to:

$$\binom{n}{k_1} \frac{k_1!(n-k_1)!}{(n+1)!} \binom{n}{k_2} \frac{k_2!(n-k_2)!}{(n+1)!} \binom{n}{k_3} \frac{k_3!(n-k_3)!}{(n+1)!} = \frac{1}{(n+1)^3}$$

The analysis will focus on the following two-tier majority mechanism:

$$Maj_2(X) = Maj_1(Maj_1(X^1), Maj_1(X^2), Maj_1(X^3)),$$

where for any vector Y in $\{L, R\}^m$ (where m is an arbitrary odd integer¹⁴) $Maj_1(Y)$ describes the outcome resulting from the popular vote in this population of m voters i.e. $Maj_1(Y) = L$ iff a majority of the m voters vote left; in each district $j = 1, 2, 3$, X^j denotes the sub-profile of preferences of voters from district j . As already pointed out Maj_2 can receive two possible interpretations. In the case of the parliamentary interpretation, $Maj_1(X^1)$, $Maj_1(X^2)$ and $Maj_1(X^3)$ are the elected representatives and $Maj_2(X)$ denotes the majority color of an elected chamber of representatives: the color is left iff the majority of representatives is leftist. In the electoral college interpretation, Maj_2 is interpreted as

¹³In particular, $\Gamma(n) = (n-1)!$ if n is a positive integer.

¹⁴In our paper, we do not need to define the majority mechanism when m is an even integer.

a two-step mechanism to elect a single candidate (say the head of the executive) (either L or R): the winner is the left candidate left iff there is a majority of districts voting left. In contrast to $Maj_2(X)$, $Maj_1(X)$ represents the popular outcome.

2.2 Divided Verdict

The paper focuses on the probability of the event:

$$E \equiv \left\{ X \in \{G, D\}^{3n} : Maj_1(X) \neq Maj_2(X) \right\}$$

For any X in E , the president elected through the electoral college does not coincide with the president elected through the popular vote. Scholars have used different names to qualify this situation: inverted elections, referendum Paradox, Divided Verdict, unpopular presidential elections,...

For any $i, j \in \{1, 2, 3\}, i \neq j$ denote by $E_{ijL} (E_{ijR})$ the event describing the profiles X for which the districts i and j vote left (right) but the majority of the $3n$ voters vote right (left). If the probability model λ is symmetric across districts and across candidates, then the six events $E_{12L}, E_{13L}, E_{23L}, E_{12R}, E_{13R}$ and E_{23R} have the same mass. In such a case:

$$\lambda(E) = 6\lambda(E_{12L})$$

Hereafter, we will denote simply by F the event E_{12L} . Let us report what is known on the calculation of $\lambda(E)$ when $\lambda = IAC^*$ and $\lambda = IC$. In the general case we have :

$$\lambda(E) = 6 \sum_{k=\frac{n+1}{2}}^{n-1} \sum_{l=\frac{n+1}{2}}^{\frac{3n-1}{2}-k} \sum_{r=0}^{\frac{3n-1}{2}-k-l} \lambda(k, l, r)$$

where $\lambda(k, l, r)$ denotes the probability that k voters from district 1 vote left, l voters from district 2 vote left and r voters from district 3 vote left. In the case where $\lambda = IAC^*$, we obtain specifically:

$$\begin{aligned} \lambda(E) &= 6 \sum_{k=\frac{n+1}{2}}^{n-1} \sum_{l=\frac{n+1}{2}}^{\frac{3n-1}{2}-k} \sum_{r=0}^{\frac{3n-1}{2}-k-l} \binom{n}{k} \frac{k!(n-k)!}{(n+1)!k!(n-k)!} \binom{n}{l} \frac{l!(n-l)!}{(n+1)!} \binom{n}{k_3} \frac{r!(n-r)!}{(n+1)!} \\ &= \frac{6}{(n+1)^3} \sum_{k=\frac{n+1}{2}}^{n-1} \sum_{l=\frac{n+1}{2}}^{\frac{3n-1}{2}-k} \sum_{r=0}^{\frac{3n-1}{2}-k-l} = \frac{6}{(n+1)^3} \left(\frac{1}{48}n^3 + \frac{3}{48}n^2 - \frac{1}{48}n - \frac{3}{48} \right) \\ &= \frac{1}{8} \frac{n^3 + 3n^2 - n - 3}{n^3 + 3n^2 + 3n + 1} = \frac{(n+3)(n-1)(n+1)}{8(n+1)^3} = \frac{n^2 + 2n - 3}{8(n+1)^2} \end{aligned}$$

We deduce from above that $\lambda(E)$ tends to $\frac{1}{8} = 12.5\%$ when $n \rightarrow \infty$. Let us now consider the case where $\lambda = IC$.

Denote S^j for $j = 1, 2, 3$, the random variable $\sum_{i=1}^n X_i^j$ where $X_i^j = 1$ iff voter i in district j votes left and $X_i^j = 0$ if voter i votes right: S^j is therefore the number of voters who vote left in district j . Since S^j is the sum of independent and identically distributed Bernoulli random variables of parameter $\frac{1}{2}$, we deduce from the central limit theorem that if n is large the law of $\frac{S^j - \frac{n}{2}}{\frac{\sqrt{n}}{2}}$ is approximately the law of a unit Gaussian $N(0, 1)$. Similarly, the law of $\frac{S - \frac{3n}{2}}{\frac{\sqrt{3n}}{2}}$ where $S = S^1 + S^2 + S^3$ is also approximately the law of a unit Gaussian. Since the event F is described by the inequalities:

$$\begin{aligned} S^1 &> \frac{n}{2} \\ S^2 &> \frac{n}{2} \\ S &< \frac{3n}{2} \end{aligned}$$

we deduce from the multivariate central limit theorem that when n is large, $\lambda(F)$ is approximately the probability mass $\mu(F)$ of the area of \mathbb{R}^3 described by the inequalities:

$$\begin{aligned} Z^1 &> 0 \\ Z^2 &> 0 \\ Z^1 + Z^2 + Z^3 &< 0 \end{aligned}$$

where $Z = (Z_1, Z_2, Z_3)$ is a Gaussian vector with mean vector equal to 0 and a variances-covariances matrix equal to identity. The exact value of $\mu(F)$ has been derived by Feix, Lepelley, Merlin and Rouet (2004):

$$\mu(F) = \frac{\text{Arc cos}(\frac{\sqrt{3}}{3})}{2\pi} - \frac{1}{8}$$

from which we deduce that $\lambda(E)$ is approximately equal to¹⁵:

$$3 \frac{\text{Arc cos}(\frac{\sqrt{3}}{3})}{\pi} - \frac{3}{4} \simeq 0.16226$$

¹⁵We could use instead Monte-Carlo simulations to calculate the probability of the event. One idea consists in simulating long sequences $t = 1, \dots, T$ of random draws of a three dimensional vector Z distributed as $N(0, I)$. To each realization t of Z , we attach the corresponding realization of the multinomial random variable D defined by the following mutually exclusive modalities: the left wins 0 district and the popular vote, the left wins 1 district and the popular vote, the left wins 2 districts and the popular vote, the left wins three districts and the popular vote, the left wins 0 district and loses the popular vote, the left wins 1 district and loses the popular vote, the left wins 2 districts and loses the popular vote, the left wins three districts and loses the popular vote. The fourth and eighth events are empty and have therefore zero probability. According to the Glivenko-Cantelli theorem, the empirical distribution of D (defined by the eight dimensional vector of empirical frequencies) almost surely converges weakly to the true distribution of D .

2.3 The Probability of a Divided Verdict for IAC

The main purpose of this paper is to complete the above picture by offering a computation of $\lambda(E) = 6\lambda(F)$ when λ is the IAC probability model. Under IAC, we obtain

$$\begin{aligned}\lambda(F) &= \int_0^1 \sum_{k=\frac{n+1}{2}}^{n-1} \sum_{l=\frac{n+1}{2}}^{\frac{3n-1}{2}-k} \sum_{r=0}^{\frac{3n-1}{2}-k-l} \binom{n}{k} \binom{n}{l} \binom{n}{r} p^k (1-p)^{n-k} p^l (1-p)^{n-l} p^r (1-p)^{n-r} dp \\ &= \int_0^1 \sum_{k=\frac{n+1}{2}}^{n-1} \sum_{l=\frac{n+1}{2}}^{\frac{3n-1}{2}-k} \sum_{r=0}^{\frac{3n-1}{2}-k-l} \binom{n}{k} \binom{n}{l} \binom{n}{r} p^{k+l+r} (1-p)^{3n-k-l-r} dp\end{aligned}$$

which by using (1) simplifies to:

$$\lambda(F) = \sum_{k=\frac{n+1}{2}}^{n-1} \sum_{l=\frac{n+1}{2}}^{\frac{3n-1}{2}-k} \sum_{r=0}^{\frac{3n-1}{2}-k-l} \binom{n}{k} \binom{n}{l} \binom{n}{r} \frac{(k+l+r)!(3n-k-l-r)!}{(3n+1)!} \quad (2)$$

In what follows, we will denote $\phi(n)$ the right hand-side of (2)

$$\phi(n) = 6 \sum_{k=\frac{n+1}{2}}^{n-1} \sum_{l=\frac{n+1}{2}}^{\frac{3n-1}{2}-k} \sum_{r=0}^{\frac{3n-1}{2}-k-l} \binom{n}{k} \binom{n}{l} \binom{n}{r} \frac{(k+l+r)!(3n-k-l-r)!}{(3n+1)!}$$

where n is an odd integer.

3 The Numerical Analysis of the Function ϕ

The main purpose of this section is to proceed to a numerical approach of the computation of $\phi(n)$ for a large but of course bounded set of values of n . The main goal of that analysis is to infer from these results the general behavior of $\phi(n)$ when n gets arbitrarily large. The numerical analysis will proceed in a sequence of steps that we now explain. First, we will proceed to a rewriting of $\phi(n)$, as factorials in the binomial coefficients lead quickly to very large numbers. The binomial coefficients which appear in $\phi(n)$ have a triple superscript, suggesting that (on top of their intrinsic size) we would have to compute about n^3 of them. To save computing time, we develop (section 3.3) a simplified algorithm which comes together with a lower bound and an upper bound which helps a lot in understanding the asymptotics. To build up this simplified algorithm, we take advantage of the binomial coefficients which show up in the summation. The first simplification of $\phi(n)$ takes advantage of the symmetry and reduces by a factor of 2 the number of computations. But the other properties of the binomial coefficients lead (section 3.4) to very useful lower and upper bounds for which the number of computations decreases from n^3 to n . We then move to approximations ϕ_{min} and ϕ_{maj} of both the lower and

the upper bounds based on the simple idea that values below some given very small threshold ε should be deleted in the sum. This leads consecutively to approximations of the two bounds as well of course to an ultimate approximation $\tilde{\phi}$ of ϕ , the number of computations and an estimate of the error. The results are reported in section 3.5 where the computations have been performed for many non adjacent values of n ranging from 3 to 10^8 with a very small ε . All numerical results confirm that $\phi(n)$ tends to 0 as $\frac{1}{\sqrt{n}}$. They suggest that $\sqrt{n}\phi(n)$, $\sqrt{n}\tilde{\phi}(n)$, $\sqrt{n}\phi_{\min}(n)$ and $\sqrt{n}\phi_{maj}(n)$ tend respectively to 0.131, 0.131, 0.061 and 0.317 when n tends to ∞ .

3.1 Rewriting of the Function

When n increases, the computation of the binomial coefficients and factorials tend quite rapidly towards infinite values (for instance, $150! \simeq 5.7 \times 10^{262}$). By using the R software, we cannot manipulate numbers beyond 1.797693×10^{308} approximatively. To make the computation feasible for relative large values of n , we first rewrite the function ϕ as follows:

$$\phi(n) = 6 \sum_{k=\frac{n+1}{2}}^{n-1} \sum_{l=\frac{n+1}{2}}^{\frac{3n-1}{2}-k} \sum_{r=0}^{\frac{3n-1}{2}-k-l} B^{k,l,r}$$

with:

$$\begin{aligned} B^{k,l,r} = & \exp(3 \ln \Gamma(n+1) + \ln \Gamma(k+l+r+1) + \ln \Gamma(3n-k-l-r+1) \\ & - \ln \Gamma(k+1) - \ln \Gamma(n-k+1) - \ln \Gamma(l+1) - \ln \Gamma(n-l+1) \\ & - \ln \Gamma(r+1) - \ln \Gamma(n-r+1) - \ln \Gamma(3n+1+1)) \end{aligned}$$

3.2 Properties of the Function $\ln \Gamma$

To compute ϕ , we need to know the values of $\ln \Gamma$ for the integers ranging from 1 to $3n+2$.

3.2.1 Algorithm

- For $n < 12$, we have used the following recursivity formula:

$$\begin{aligned} \ln \Gamma(1) &= 0 \\ \ln \Gamma(n+1) &= \ln(n) + \ln \Gamma(n) \end{aligned}$$

- For $n \geq 13$, we have used Stirling's formula (see appendix B) which ensures to keep a good machine accuracy even for large values of n :

$$\ln \Gamma(n) = \frac{1}{2} \times \ln(2\pi) + (n - \frac{1}{2}) \times \ln(n) - n + w(n) \quad (3)$$

where:

$$w(n) = \frac{1}{12n} \mathbf{1}_{n < 8943979} - \frac{1}{360n^3} \mathbf{1}_{n < 1456} + \frac{1}{1260n^5} \mathbf{1}_{n < 123} - \frac{1}{1680n^7} \mathbf{1}_{n < 37} + \frac{1}{1188n^9} \mathbf{1}_{n < 19}$$

3.2.2 Use

We have programmed in C the function `loggamma`. The values of $\ln \Gamma$ are computed before the computation of ϕ and stored in a vector of size $3n + 2$ in order to avoid computational repetition in each loop of ϕ . The figure 1 represents $\ln \Gamma$ for all integer values which are used in the computation of ϕ until 100 000 001.

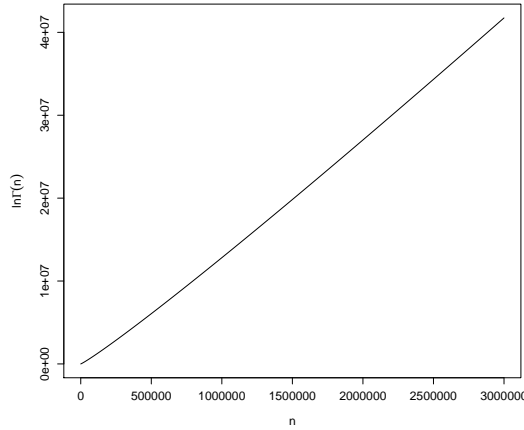


Figure 1: Values of $\ln \Gamma$ for integers.

3.3 Simplified Algorithm

The main objective of this subsection is to simplify the way to express ϕ in order to save as much as possible on computing time. In doing so, we will also propose a lower bound and an upper bound of the function ϕ which will lead to a relatively low computing time for large values of n and a good understanding of the asymptotics.

3.3.1 Initial Number of Computations

The computation of ϕ amounts to the computation of $B^{k,l,r}$ for different values of k , l and r . This number of values, of the order n^3 , is equal to:

$$\frac{1}{6}(n_2 - 1)n_2(n_2 + 1), \quad (4)$$

where $n_2 = \frac{(n+1)}{2}$. For instance when $n = 10\,001$, we would need to calculate the expression $B^{k,l,r}$ 20 845 835 000 times. The objective is to reduce as much as we can this number without losing on the quality of the outcome.

3.3.2 Few Properties of $B^{k,l,r}$

For $n = 13$, we have represented in figure 2 the values of k , l and r for which we calculate $B^{k,l,r}$. In general this coefficient satisfies a number of properties some of them are reported below¹⁶.

- P1. $B^{k,l,r} = B^{l,k,r}$
- P2. $B^{k,l,r} > B^{k,l,r-1}$ (for all feasible values of k , l , r and $r - 1$)
- P3. $B^{k,l,r} > B^{k+1,l,r}$ (for all feasible values of k , l , r and $k + 1$)
- P4. $B^{k,l,r} > B^{k,l+1,r}$ (for all feasible values of k , l , r and $l + 1$)
- P5. For each fixed value of r , the largest $B^{k,l,r}$ is obtained for $k = l = n_2 (= \frac{n+1}{2})$
- P6. $\forall l \geq k, B^{k,l,r} > B^{k-1,l+1,r}$ (for all feasible values of k , $k - 1$, l , $l + 1$ and r)
- P7. For each fixed value of r , the smallest $B^{k,l,r}$ is obtained for $k = n - 1 - r$ and $l = n_2$

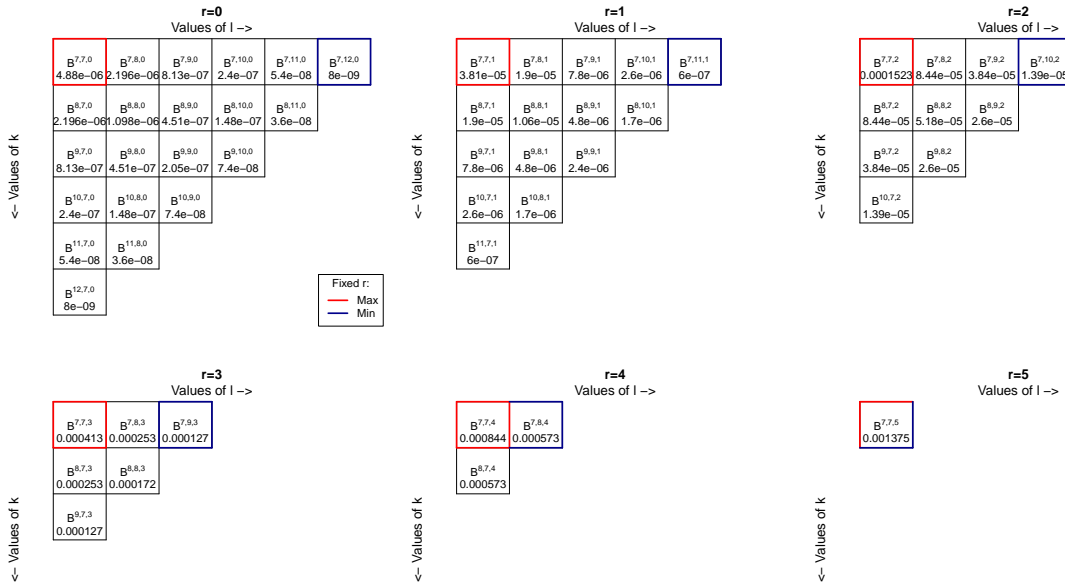


Figure 2: Representation of the $B^{k,l,r}$ used in the computation of $\phi(13)$ without any simplification. For each r , the red cell contains the maximum value and the blue cell the minimum.

¹⁶Proofs are provided in appendix A.

Remark: If we pile up the 6 levels of figure 2, we obtain a geometric pattern close to a tetrahedron. When we compute ϕ for the following value of n , we add to the tetrahedron a ground level with a number of new entries to compute equal to $n_2 \times (n_2 - 1)/2$. Note that when n increases, the values $B^{k,l,r}$ will decrease and converge to 0. For instance, on the top $B^{n_2,n_2,n_2-2} = O(n^{-2})$. The values on low levels converge even more rapidly towards 0. For instance, for the ground level ($r = 0$), $B^{n_2,n_2,0} = O(n^{-1.5} (\frac{16}{27})^n)$.

3.3.3 Simplification of ϕ

By exploiting the symmetry property (P1), we can rewrite ϕ as follows :

$$\phi(n) = 6 \times \left[2 \times \left(\sum_{k=\frac{n+1}{2}}^{n-1} \sum_{l=k+1}^{\frac{3n-1}{2}-k} \sum_{r=0}^{\frac{3n-1}{2}-k-l} B^{k,l,r} \right) + \left(\sum_{k=\frac{n+1}{2}}^{n_3} \sum_{r=0}^{\frac{3n-1}{2}-2k} B^{k,k,r} \right) \right], \quad (5)$$

where $n_3 = \frac{3n-1}{4} \mathbf{1}_{\{n_2 \text{ even}\}} + \frac{3n-3}{4} \mathbf{1}_{\{n_2 \text{ odd}\}}$

For $n = 13$, we have represented in figure 3 the computations which have been save through the use of this symmetry property. The cells on the diagonal (represented in magenta) correspond to the computation on the right-side of equation 5.

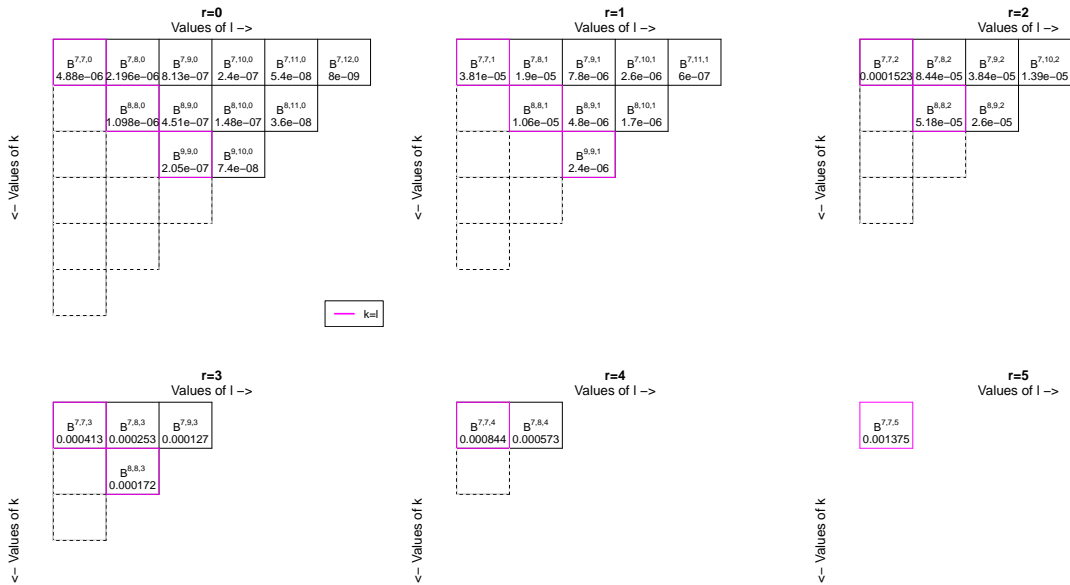


Figure 3: Representation of the $B^{k,l,r}$ used in the computation of $\phi(13)$ after simplification. The cells on the diagonal (represented in magenta) correspond to the computation on the right-side of equation 5.

The number of computations to be done numerically has been almost divided by 2, but remains of the order of n^3 . Precisely this number is equal to:

$$C(n) = \begin{cases} \frac{1}{24}n_2(n_2+2)(2n_2-1) & \text{if } n_2 \text{ is even} \\ \frac{1}{24}(n_2-1)(n_2+1)(2n_2+3) & \text{if } n_2 \text{ is odd} \end{cases}$$

For instance, when $n = 10\,001$, we would need now to calculate the expression $B^{k,l,r}$ 10 426 043 750 times, leading to a relative gain by a factor 1.9994 when compared to the previous one.

3.4 Lower and Upper Bounds on ϕ

By exploiting properties P5 and P7, we obtain the following of the function ϕ :

$$\phi_{min} \leq \phi \leq \phi_{maj},$$

where:

$$\phi_{maj}(n) = 6 \sum_{r=0}^{n_2-2} \frac{1}{2} (n_2 - r - 1)(n_2 - r) B^{n_2, n_2, r} \quad (6)$$

and:

$$\phi_{min}(n) = 6 \sum_{r=0}^{n_2-2} \frac{1}{2} (n_2 - r - 1)(n_2 - r) B^{n-1-r, n_2, r}$$

which can be expressed equivalently through the change of variable $k = n - 1 - r$, as:

$$\phi_{min}(n) = 6 \sum_{k=n_2}^{n-1} \frac{1}{2} (k - n_2 + 2)(k - n_2 + 1) B^{k, n_2, (n-1-k)}$$

which will be very useful in what follows (see 3.4.2).

The number of computations for ϕ_{maj} and ϕ_{min} is of order n (in contrast to n^3 for ϕ).

On the other hand, as explained before, the values of the coefficients $B^{k,l,r}$ tend to 0 when n gets large and this decrease is faster at the ground levels of the tetrahedron as compared to the upper levels. Therefore, it is even possible to reduce further the number of computations without altering the accuracy of the overall computation.

3.4.1 Approximation of ϕ_{maj} and ϕ_{min}

Intuition for an approximation of ϕ_{maj} : When n increases and r tends to 0, the coefficient $B^{n_2, n_2, r}$ tends to 0 (and will be then considered to be equal to 0 by \mathbb{R} when around $2.225074 \times 10^{-308}$). The main idea to simplify the algorithm is to postulate that we will compute $B^{n_2, n_2, r}$ only for values of r such that $B^{n_2, n_2, r}$ is above a threshold considered to be reasonable.

Let r_{min} , be the smallest integer value largest than or equal to 0, such that if $r \geq r_{min}$, then $B^{n_2, n_2, r} > \varepsilon$ where ε is the fixed degree of accuracy which we impose. We approximate ϕ_{maj} as follows:

$$\tilde{\phi}_{maj}(n) = 6 \sum_{r=r_{min}}^{n_2-2} \frac{1}{2} (n_2 - r - 1)(n_2 - r) B^{n_2, n_2, r}$$

The error due to approximation resulting from $\tilde{\phi}_{maj}$ rather than ϕ_{maj} is:

$$Err_1 = \begin{cases} 6 \sum_{r=0}^{r_{min}-1} \frac{1}{2} (n_2 - r - 1)(n_2 - r) B^{n_2, n_2, r} & \text{if } r_{min} > 0 \\ 0 & \text{otherwise} \end{cases}$$

Intuition for an approximation of ϕ_{min} : The idea is the same as before. The coefficient $B^{k, n_2, (n-1-k)}$ converges to 0 when n gets large and k tends to $n-1$. More precisely, the idea is to compute $B^{k, n_2, (n-1-k)}$ only for the k for which $B^{k, n_2, (n-1-k)}$ is above the threshold which is above degree of accuracy which we impose.

Let k_{max} , be the largest integer smallest than or equal to $(n-1)$, defined such that if $k \leq k_{max}$, then $B^{k, n_2, (n-1-k)} > \varepsilon$. We approximate ϕ_{min} as follows:

$$\tilde{\phi}_{min}(n) = 6 \sum_{k=n_2}^{k_{max}} \frac{1}{2} (k - n_2 + 2)(k - n_2 + 1) B^{k, n_2, (n-1-k)}$$

The error due to approximation resulting from $\tilde{\phi}_{min}$ rather than ϕ_{min} is:

$$Err'_1 = \begin{cases} 6 \sum_{k=k_{max}+1}^{n-1} \frac{1}{2} (k - n_2 + 2)(k - n_2 + 1) B^{k, n_2, (n-1-k)} & \text{if } k_{max} < n-1 \\ 0 & \text{otherwise} \end{cases}$$

Hereafter, the C corresponding functions are called IAC_{maj} and IAC_{min} . In addition to the values of n that he wants to consider for the computation, the user will have to fix the degree of accuracy ε . Moreover, the functions C return in addition to $\tilde{\phi}_{maj}$ and $\tilde{\phi}_{min}$, the approximation errors Err_1 and Err'_1 , as well as r_{min} and k_{max} . This would allow us to pick up ε in order to control Err_1 and Err'_1 .

Remark: The outcome for ϕ_{maj} (resp. ϕ_{min}) is identical to the outcome for $\tilde{\phi}_{maj}$ (resp. $\tilde{\phi}_{min}$) with $\varepsilon = 2.225074 \times 10^{-308}$, since this value of ε is the smallest value recognizable by R. In contrast, the number of computations involved for $\tilde{\phi}_{maj}$ (resp. $\tilde{\phi}_{min}$) is always smaller than the number involved for ϕ_{maj} (resp. ϕ_{min}). In order to save computation time, while keeping as much as possible $B^{k, l, r}$, it is

therefore always better to run the computations in considering $\tilde{\phi}_{maj}$ (resp. $\tilde{\phi}_{min}$), with $\varepsilon = 2.225074 \times 10^{-308}$. This turns to be useful quite rapidly: as soon as $n \geq 1401$ for $\tilde{\phi}_{maj}$ (before, $r_{min} = 0$), even as soon as $n \geq 539$ for $\tilde{\phi}_{min}$ (before, $k_{max} = n - 1$). We deduce then wrongly that: $Err_1 = Err'_1 = 0$. The errors resulting from the granularity of the values recognizable by \mathbb{R} are discussed with further details in section 3.6. Note however that the number of $B^{k,l,r}$ below that ε (and therefore considered equal to 0) is less than the total number of $B^{k,l,r}$ (which is of the order $\frac{n^3}{48}$; see equation 4). Furthermore, we will see (see section 3.5.1) that $\phi_{min}(n)$ gets close to $\frac{0.06}{\sqrt{n}}$ i.e. $6 \times 10^{-(p+2)}$, when $n = 10^{2p} + 1$. Since the granularity of \mathbb{R} leads at best to 16 significant digits, we target an accuracy corresponding to $10^{-(p+19)}$. Therefore, it is sufficient that $\frac{n^3}{48} \times \varepsilon$ which is less than 10^{6p-306} be smaller than $10^{-(p+19)}$. This happens when $p \leq \frac{287}{7} = 41$. Accordingly, getting wrongly $Err_1 = Err'_1 = 0$ is without any consequence at least when n is less than $10^{82} + 1$; and we will see that we stop long before reaching that value!

3.4.2 Approximation of ϕ

Approximation 1 In using r_{min} and k_{max} as defined before, we approximate ϕ as follows:

$$\tilde{\phi}_0(n) = 6 \times \left[2 \times \left(\sum_{k=\frac{n+1}{2}}^{k_{max}} \sum_{l=k+1}^{l_{max}} \sum_{r=r_{min}}^{r_{max}} B^{k,l,r} \right) + \left(\sum_{k=\frac{n+1}{2}}^{k'_{max}} \sum_{r=r_{min}}^{r'_{max}} B^{k,k,r} \right) \right]$$

where $l_{max} = \min(\frac{3n-1}{2} - k, k_{max})$, $r_{max} = \frac{3n-1}{2} - k - l$, $k'_{max} = \min(n_3, k_{max})$ and $r'_{max} = \frac{3n-1}{2} - 2k$. The approximation error resulting from considering $\tilde{\phi}_0$ instead of ϕ is lower than $Err_1 + Err_2$, with:

$$Err_2 = \begin{cases} 6 \sum_{k=k_{max}+1}^{n-1-r_{min}} \frac{1}{2} (k_{max} - k)(k_{max} - k + 1) B^{k, n_2, (n-1-k)} & \text{if } k_{max} < n - 1 - r_{min} \\ 0 & \text{otherwise} \end{cases}$$

For the case where $n = 13$, we have represented in figure 4 the computations which have been avoided with the help of that approximation when $\varepsilon = 2 \times 10^{-5}$. In that example, we find $r_{min} = 1$ and $k_{max} = 9$.

Remark: In considering $\varepsilon = 2 \times 10^{-5}$, we observe that when $r = 1$, we keep counting the cells whose value is lower than ε . The next idea to improve on approximation is to delete these cells.

Approximation 2 Let r_{kl} , be defined such that for fixed k and l , $B^{k,l,r} > \varepsilon$ for all $r > r_{kl} \geq r_{min}$. Then:

$$\tilde{\phi}(n) = 6 \left[2 \times \left(\sum_{k=\frac{n+1}{2}}^{k_{max}} \sum_{l=k+1}^{l_{max}} \sum_{r=r_{kl}}^{r_{max}} B^{k,l,r} \right) + \left(\sum_{k=\frac{n+1}{2}}^{k'_{max}} \sum_{r=r_{kk}}^{r'_{max}} B^{k,k,r} \right) \right]$$

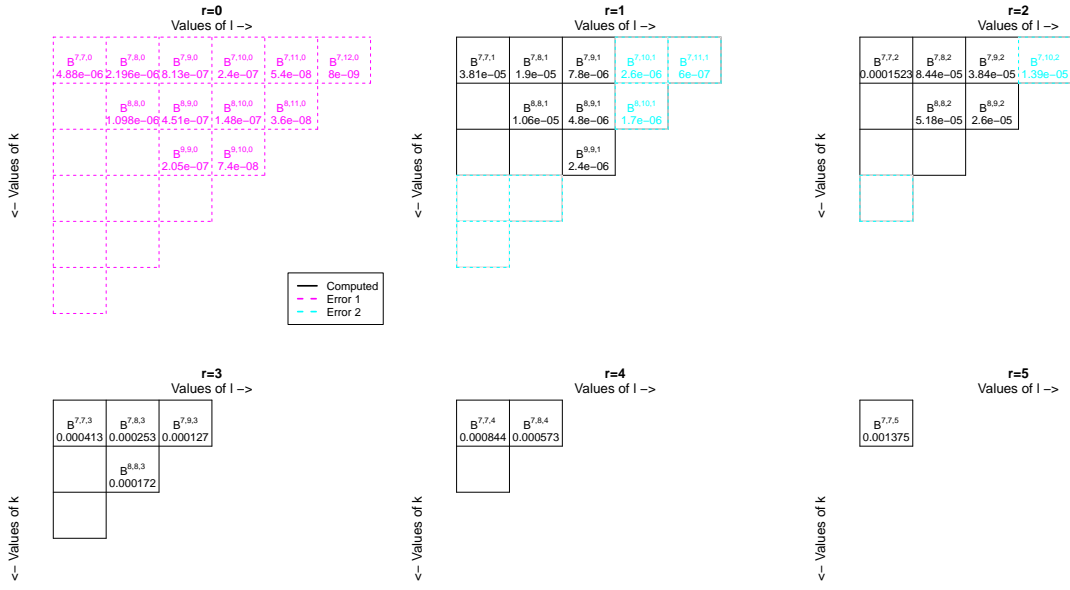


Figure 4: Representation of the $B^{k,l,r}$ used in the computation of $\phi(13)$ after a first approximation, with $\varepsilon = 2 \times 10^{-5}$. In this case $r_{min} = 1$ (sparing the computation of the magenta dotted cells) and $k_{max} = 9$ (sparing the computation of the blue dotted cells).

The approximation error resulting from considering $\tilde{\phi}$ instead of $\tilde{\phi}_0$ is less than:

$$Err_3 = \varepsilon \times 6 \left[2 \times \left(\sum_{k=\frac{n+1}{2}}^{k_{max}} \sum_{l=k+1}^{l_{max}} (r_{kl} - r_{min}) \right) + \left(\sum_{k=\frac{n+1}{2}}^{k'_{max}} (r_{kk} - r_{min}) \right) \right]$$

When $n = 13$, we have represented in figure 5 in orange the computations which have been avoided as a consequence of that second approximation (still when $\varepsilon = 2 \times 10^{-5}$). In that example, we get: $r_{78} = r_{79} = r_{88} = r_{89} = r_{99} = 2$. This is the expression¹⁷ which has been used to code the function labeled *IAC* in C (see an illustration of its use in D).

¹⁷Truly in coding the function, we have reversed the order of summation on k, l and r in order to arrange the $B^{k,l,r}$ in an increasing order. Without that, we could add further accuracy errors in computing $\tilde{\phi}$.

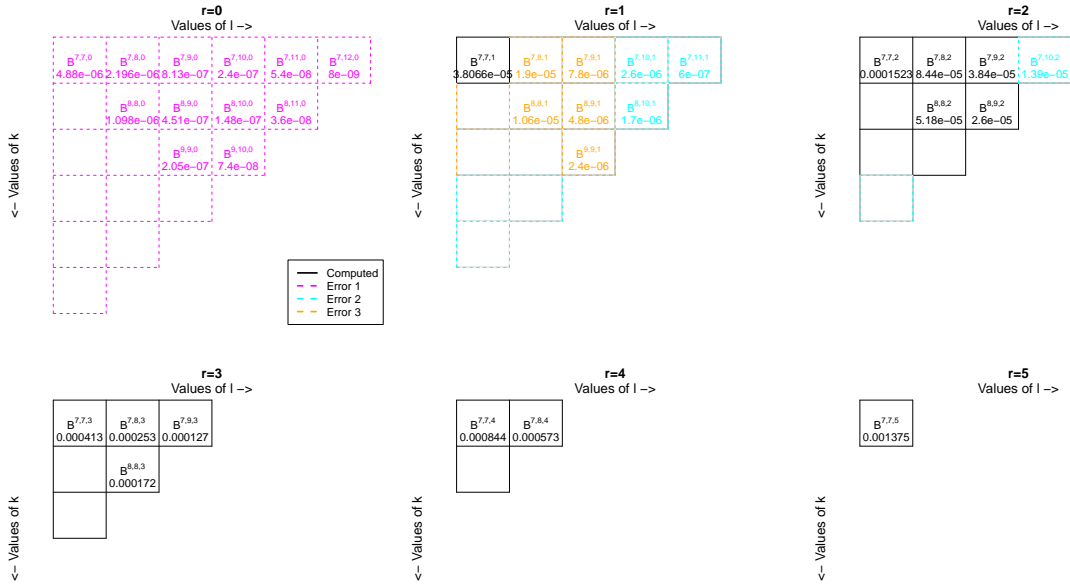


Figure 5: Representation of the $B^{k,l,r}$ used in the computation of $\phi(13)$ after a second approximation, with $\varepsilon = 2 \times 10^{-5}$. In this case $r_{78} = r_{79} = r_{88} = r_{89} = r_{99} = 2$ (sparing the computation of the orange dotted cells).

3.4.3 Ultimate Number of Computations

The total number of computations corresponds to the number of times the expression $B^{k,l,r}$ has been computed. This implies:¹⁸:

$$Nb_{calc} = \sum_{k=\frac{n+1}{2}}^{k_{max}} \sum_{l=k+1}^{l_{max}} (r_{max} - r_{kl} + 2) + \sum_{k=\frac{n+1}{2}}^{k'_{max}} (r'_{max} - r_{kk} + 2) + n - 1 - k_{max}$$

We have represented in figure 6 the number of times we have to calculate the expression $B^{k,l,r}$ as a function of n , for several values of ε . We have also represented the number of computations in the case where we do no approximation of order n^3 (equation 3.3.3) and in the case where we compute ϕ_{maj} of order n . The scale units are in \log_{10} to ease the reading of the representation. We observe that for all the first values of n ($n < 21$), there is no saving in computation since all the values of $B^{k,l,r}$ are larger than ε . In contrast when $n = 10^8 + 1$, the number of computations needed for ϕ is of the order 10^{22} while it is only of the order 10^{12} for $\tilde{\phi}$ when $\varepsilon = 10^{-25}$ and of the order 10^{11} when $\varepsilon = 10^{-20}$. If we

¹⁸Here, we report the number of computations which also allow to provide an estimate of the error in approximation. If we were not interested by the error in approximation, we could make some extra saving by substituting 2 to $n - 1 - k_{max}$ in the formula.

compute $\tilde{\phi}$ by taking $\varepsilon = 10^{-15}$, we observe that when n is larger than $2 \times 10^7 + 1$, all the expressions $B^{k,l,r}$ are smaller than the threshold and the number of computations collapses to 0^{19} . But, $Err = Err_1 > \phi(n)$. Precisely, $\phi(2 \times 10^7 + 1) \approx 3 \times 10^{-5}$, with $Err = Err_1 \approx 7 \times 10^{-5}$. More generally, we will see in appendix B that the cell with the largest value (the peak of the tetrahedron) behaves as: $B^{n_2, n_2, n_2-2} = \frac{2}{\sqrt{3}\pi n^2} - O\left(\frac{1}{n^3}\right)$. Therefore, if $n = 10^p + 1$ and $\varepsilon = 10^{-q}$, then the approximation returns 0 as the outcome when $\varepsilon > B^{n_2, n_2, n_2-2}$, with $B^{n_2, n_2, n_2-2} < 10^{-2p-0.434}$, i.e. at least for $q < 2p + 0.434$. For instance, this happens when $q = 15$, as soon as $p > 7.283$, i.e. $n > 1.92 \times 10^7$ and when $q = 20$ as soon as $n > 6.07 \times 10^9$. Note also that for any given ε , the value of $\tilde{\phi}$ diverges from the value of ϕ long before reaching these limit values of n (see section 3.4.4).

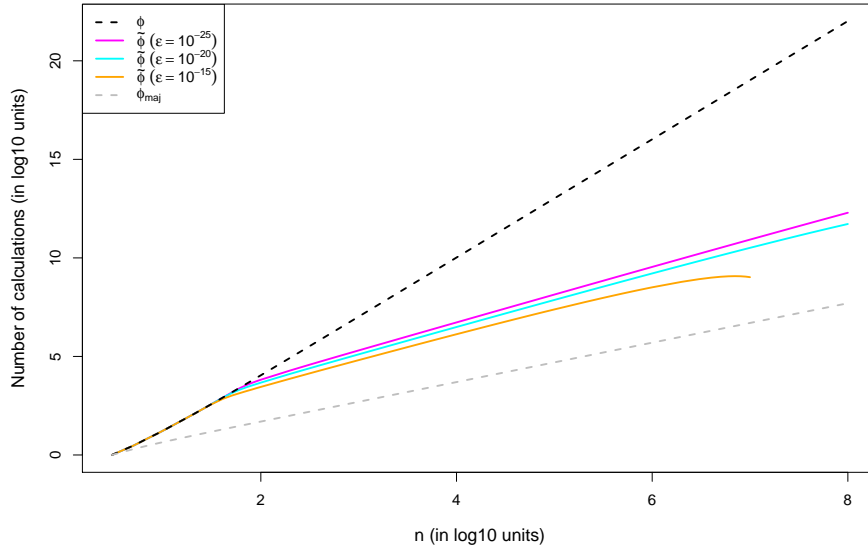


Figure 6: Number of $B^{k,l,r}$ computations necessary to compute ϕ , $\tilde{\phi}$ with $\varepsilon = 10^{-25}, 10^{-20}, 10^{-15}$ and ϕ_{maj} according to the value of n .

3.4.4 Approximation Error

We have pointed out that computing $\tilde{\phi}$, instead of ϕ , saves the calculation of many $B^{k,l,r}$. As a result, these expressions disappear from the computation of ϕ . The approximation error in moving from ϕ to $\tilde{\phi}$ is at most:

$$Err = Err_1 + Err_2 + Err_3$$

¹⁹In fact a unique calculation, the cell on the top of the tetrahedron B^{n_2, n_2, n_2-2} , which leads to find that $r_{max} > n_2 - 2$ and therefore that no cell appears in the computation of the approximation of ϕ which is then considered to be equal to 0.

Figure 7 represents the approximation errors by taking $\tilde{\phi}$ instead of ϕ with respect to n for the following values of ε : 10^{-25} , 10^{-20} , 10^{-15} . For small values of n , the approximation error vanishes²⁰. Usually, the approximation errors increase as n increases. For instance, when $n = 10^6 + 1$, the approximation error is of the order of 10^{-15} , 10^{-11} and 10^{-6} for $\varepsilon = 10^{-25}$, 10^{-20} , 10^{-15} . Interestingly, whatever the choice of ε , after a short period of great increase of the approximation error (from 0 to $\varepsilon \times 10^5$ when n increases), the increase seems to be linear (in \log_{10} scales) and the steps of those lines seem to be very close from one ε to another: around 1.5. This comes from previous figure 6: The number of avoided computations has a steep of 1.5 or so (in \log_{10} scales): step difference between the black dotted line and the colored ones. So if you multiply the number of avoided computations by ε , you get a good proxy of the approximation error.

Of course, the orange line ($\varepsilon = 10^{-15}$) deviates for large values of n . This has partly been explained when commenting the previous figure: For $n > 1.92 \times 10^7$, the approximation error (with this ε) is larger than the value of $\phi(n)$, $\tilde{\phi}(n) = 0$ and $Err = Err_1 = \phi_{maj}(n)$. As it has been shown (though not formally proved) that $\phi_{maj}(n)$ converges to 0 (see section 3.5.1), it is logical that the approximation error tends towards 0, once it is above the true value of $\phi(n)$.

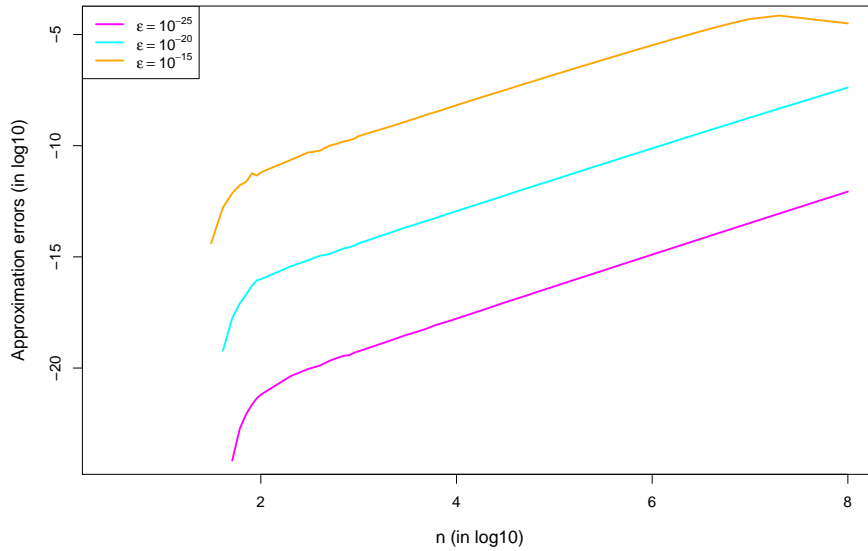


Figure 7: Approximation errors when computing $\tilde{\phi}$ instead of ϕ , with $\varepsilon = 10^{-25}$, 10^{-20} and 10^{-15} according to n .

²⁰In the sense that all the $B^{k,l,r}$ are calculated. Then, $\tilde{\phi} = \phi$. It remains numerical errors attached to the computations but there are negligible.

3.4.5 Parallelization of Function ϕ

To save on computing time, we have proceeded in parallel computing of $\tilde{\phi}$ i.e. we have computed $\tilde{\phi}$ piecewise. Otherwise stated, we have spread the computation of $\tilde{\phi}$ on several cores²¹. To do so, we send onto the core i , $i = 1, \dots, nbc$, where nbc is the total number of available cores, the computation of $\tilde{\phi}$ for the set of values $\{k, \text{ such that: } k = (\frac{n+1}{2} + i - 1) + npc \times j \leq k_{max}, \text{ with } j = 1, 2, \dots\}$, based on the idea that the number of computations on each core is more or less the same. For instance the computation of $\tilde{\phi}(1\ 000\ 001)$ for $\varepsilon = 10^{-25}$ took a bit less than 56s by using 4 cores (instead of 222s with a unique core). The function coded in C is called `IAC_par`. For the computations of ϕ or $\tilde{\phi}$, we have been using up to 50 cores.

3.5 Results

In this section, the computations have been performed for 68 non adjacent values of n ranging from 1 to 100 000 001. Precisely, we have selected the following values of n : 3, 5, 7, 9, then 11, 21, ..., 91, then 101, 201, ..., 901, then 1 001, 2 001, ..., 9 001, then 10 001, 20 001, ..., 90 001, then 100 001, 200 001, ..., 900 001, then 1 000 001, 2 000 001, ..., 9 000 001, then 10 000 001, 20 000 001, ..., 90 000 001 and finally 100 000 001. Further, we decided to display the results in the case where $\varepsilon = 10^{-25}$, which guarantees an approximation error quite negligible with respect to the differences between two consecutive values (in the sequence of 68 integers n which are considered) for $\phi(n) \times \sqrt{n}$.

3.5.1 ‘Intuitive’ Limit of ϕ

We have represented in figure 8, $\tilde{\phi}$, $\tilde{\phi}_{min}$ and $\tilde{\phi}_{maj}$ with respect to n . We also reported on table 1, $\tilde{\phi}$, $\tilde{\phi}_{min}$ and $\tilde{\phi}_{maj}$ for a sample of values of n . Both figure 8 and table 1, suggest:

$$\lim_{n \rightarrow +\infty} \phi = 0.$$

3.5.2 ‘Intuitive’ Speed of Convergence of ϕ

Figure 9 represents $\sqrt{n} \times \tilde{\phi}_{min}$, $\sqrt{n} \times \tilde{\phi}$ and $\sqrt{n} \times \tilde{\phi}_{maj}$. It seems that ϕ tends to 0 at the same speed of convergence as $\frac{1}{\sqrt{n}}$.

²¹Nowadays, most of the computers are endowed with at least two multi-core processes. At GREMAQ, we benefit from a computer server with four processors IntelXeon CPU E7 - 4870 2.40Ghz, each with 10 physical cores (20 logic devices).

n	100 001	1 000 001	10 000 001	100 000 001
$\tilde{\Phi}_{min} \times 10^4$	1.945116	0.6121303	0.1932749	0.06108912
$\tilde{\Phi} \times 10^4$	4.139992	1.309204	0.4140074	0.1309208
$\tilde{\Phi}_{maj} \times 10^4$	9.994129	3.169424	1.003156	0.3173155

Table 1: Values of $\tilde{\Phi}$, $\tilde{\Phi}_{maj}$ and $\tilde{\Phi}_{min}$. Orange decimals could be affected by numerical precision errors (see section 3.6).

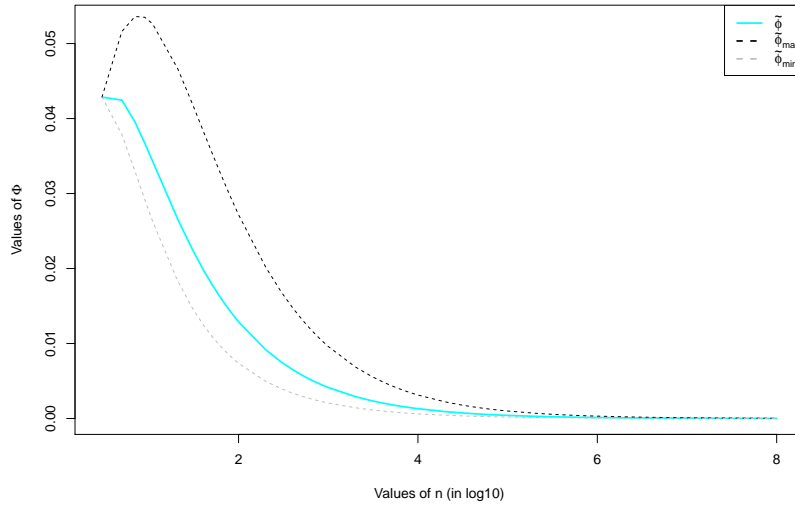


Figure 8: Representation of $\tilde{\Phi}$, $\tilde{\Phi}_{min}$ and $\tilde{\Phi}_{maj}$ according to n .

3.5.3 ‘Intuitive’ Value of $\lim_{n \rightarrow +\infty} \sqrt{n} \times \phi$

Table 2 represents $\sqrt{n} \times \tilde{\Phi}$, $\sqrt{n} \times \tilde{\Phi}_{maj}$ and $\sqrt{n} \times \tilde{\Phi}_{min}$ for a sample of values n . It suggests the following majorization and minorization:

$$\mathbf{a} = \lim_{n \rightarrow +\infty} \sqrt{n} \phi_{min} \leq \lim_{n \rightarrow +\infty} \sqrt{n} \phi = \mathbf{b} \leq \lim_{n \rightarrow +\infty} \sqrt{n} \phi_{maj} = \mathbf{c}$$

with: $a \simeq 0.06$, $b \simeq 0.131$ and $c \simeq 0.32$.

3.6 Validity of the Results

We have represented in figure 10 a zoom of $\sqrt{n} \times \tilde{\Phi}$ for large values of n . We observe that the curve is less and less smooth when n increases. We can attribute these numerical perturbations to the relative precision given by R to the float format (around 10^{-16}), which is insufficient to compute accurately $\tilde{\Phi}$ for large values of n . Then, it remains to determine until which decimals the results that we give remain valid:

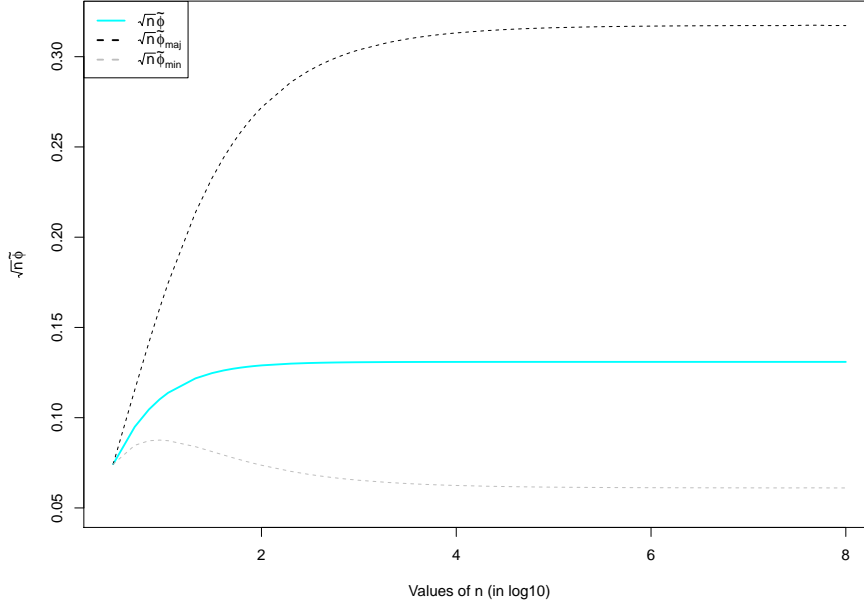


Figure 9: Representation of $\sqrt{n} \times \tilde{\phi}_{min}$, $\sqrt{n} \times \tilde{\phi}$ and $\sqrt{n} \times \tilde{\phi}_{maj}$ according to n .

n	100 001	1 000 001	10 000 001	100 000 001
$\sqrt{n}\tilde{\phi}_{maj}$	0.3160436738	0.3169426034	0.3172258387	0.3173155175
$\sqrt{n}\tilde{\phi}$	0.1309186886	0.1309204525	0.1309206294	0.1309207983
$\sqrt{n}\tilde{\phi}_{min}$	0.06151027472	0.06121305701	0.06111889019	0.06108912362

Table 2: Computation of $\sqrt{n}\tilde{\phi}$, $\sqrt{n}\tilde{\phi}_{min}$ and $\sqrt{n}\tilde{\phi}_{maj}$ for several values of n . Orange decimals could be affected by numerical precision errors (see section 3.6).

For each $B^{k,l,r}$ of the sum defining ϕ , $\ln\Gamma(3n+2)$ is the highest computed value to obtain $B^{k,l,r}$. Besides, $\ln\Gamma(3n+2)$ is of the order $3n \times \ln(n) + o(n \times \ln(n))$, see (3). So $\ln(B^{k,l,r})$ leads to the computation of value $lB^{k,l,r}$, which is only known up to $+/-u_n$ at best, where $u_n = 3n \times \ln(n) \times 10^{-16}$. Hence, $B^{k,l,r} = \exp(lB^{k,l,r} +/- u_n) = \exp(lB^{k,l,r}) * \exp(+/- u_n)$. As u_n is supposed to be small, $\exp(+/- u_n)$ can be approximated by $1 +/- u_n$. Finally, $\tilde{\phi}$, $\tilde{\phi}_{maj}$ and $\tilde{\phi}_{min}$ are only known up to a relative precision of u_n .

For instance, in Table 1, for $n = 100\,000\,001$, $u_n \simeq 10^{-6}$: so, the last digit (in orange) is +/- the first non-zero digit, and so only the digits in black are correct for sure. In fact, figure 11 shows that at this value of n , the approximation error is dominated by the relative precision of floats. Hence, the black digits in Table 1 are also correct for ϕ , ϕ_{maj} and ϕ_{min} .

Similar results hold in Table 2. Interestingly, when going to a n 10 times bigger, one digit precision is lost. For instance, in figure 10, for $n = 100\,000\,001$, the confidence interval of the true value of $n^{1/2}\tilde{\phi}$ is from 0.13092067 to 0.13092092. Similar confidence intervals hold for the other points on the

figure. So it is possible to imagine a smooth curve in the envelope formed by the confidence intervals. In fact, the represented curve in figure 10 is not smooth because the confidence intervals between two consecutive computed values of $n^{1/2}\tilde{\phi}$ are too overlapping.

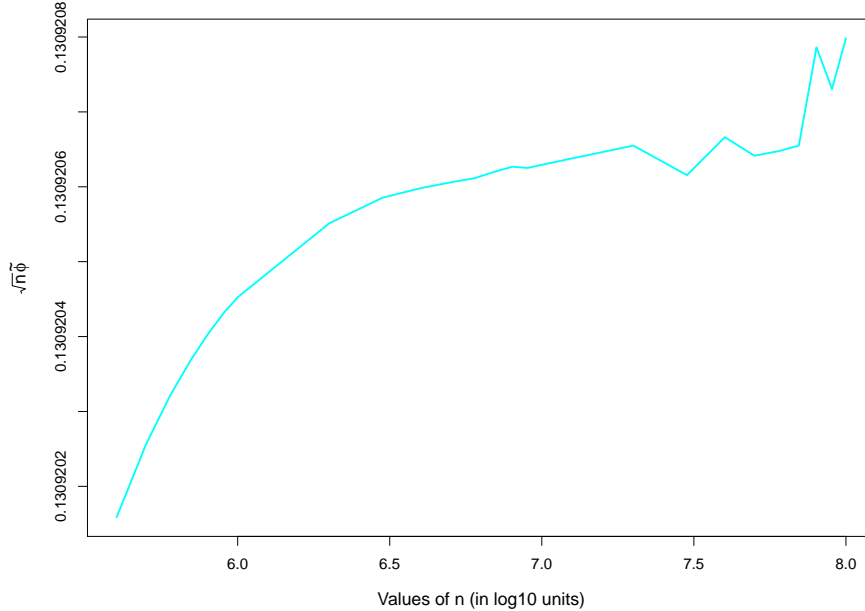


Figure 10: Zoom of $\sqrt{n} \times \tilde{\phi}$ for large values of n .

This is even better explained in figure 11: As n gets large, the difference between two consecutive computations of $n^{1/2}\tilde{\phi}$ from the considered list of values of n gets smaller, whereas the absolute numerical imprecision increases.

When those two curves cross ($\log_{10}(n) \simeq 6.4$), the numerical imprecision is of same order as the computed difference between two consecutive computations. So the computed difference conveys no information: the true difference can (at least theoretically) even be of the opposite sign of the computed difference!

The situation is even worse after $\log_{10}(n) \simeq 6.6$, where the numerical imprecision dominates the computed difference. So the absolute value of the true difference could be much bigger than the absolute value of the computed difference. This can explain why the curve of the computed difference does not follow the same pattern before and after $\log_{10}(n) \simeq 6.6$, as one could intuitively expect it to.

In fact, in order to be sure that the computed differences dominate the numerical imprecisions, computations should stop around $\log_{10}(n) \simeq 5.9$. There, the numerical imprecision is at least 10 times smaller than the computed difference. Note also that up to $\log_{10}(n) \simeq 5.6$, the numerical imprecision is at least 100 times smaller than the computed difference.

What about the approximation error between $\tilde{\phi}$ and ϕ ? Figure 11 shows that for $\epsilon = 10^{-25}$ (which has been used here for $n^{1/2}\tilde{\phi}$ computations), the maximal approximation error is always dominated by

the maximal numerical precision error. In fact, the latter is at least 100 times bigger than the former. So the approximation error is negligible and every results for $\tilde{\phi}$ hold for ϕ too.

Had ε been 10^{-20} , the maximal approximation error would have been at least 100 times smaller than the maximal numerical precision error only up to $\log_{10}(n) \simeq 2.5$. But as computation time is mainly a problem when n gets large, there is only very little interest to use a coarser ε for small values of n .

Finally, in order to have a more correct curve after $\log_{10}(n) \simeq 5.9$, one can either compute less values of n (hence, the difference between two computed values increases way above the maximal numerical precision error) or use a finer representation of floats than double precision (as quadruple precision that give at least 33 significant decimal digits instead of 15 for double precision).

Yet, a finer representation also implies more computing time. This does not seem necessary for this paper, as the results with double precision floats have already been shown valid up to $n = 100\,000\,001$ with 6 significant decimal digits. This numerical approach is mainly interesting in the sense that it gives intuitions on the speed of convergence thanks to results that are valid.

The following section builds on this intuition to give analytical bounds for the speed of convergence of ϕ .

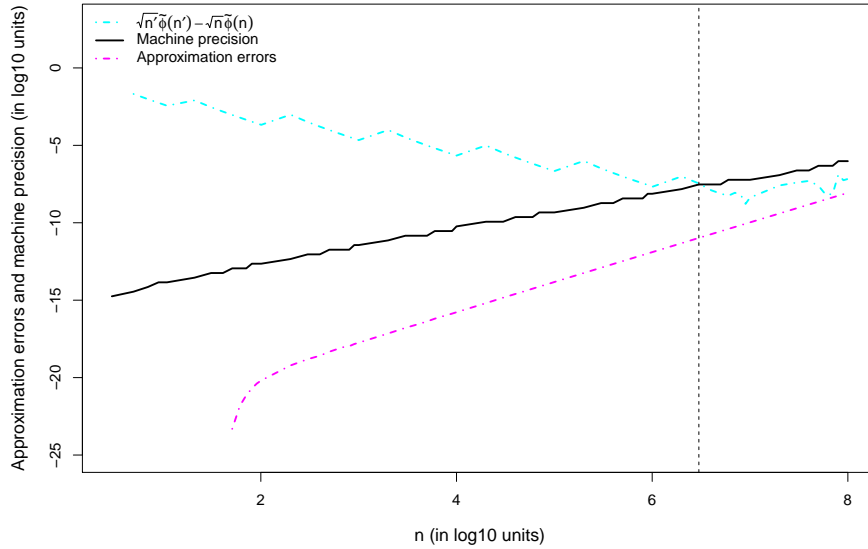


Figure 11: Representation according to n of the maximum approximation error (for $\varepsilon = 10^{-25}$), the maximal numerical imprecision error (due to machine precision limitations) and the difference between two consecutive computations from the considered list: $\sqrt{n'} \times \tilde{\phi}(n') - \sqrt{n} \times \tilde{\phi}(n)$, where n' is the value that follows n in the list of considered values.

4 Analytical Results on the Speed of Convergence of $\phi(n)$ Towards 0

In the preceding section we have introduced a lower and an upper bound of $\phi(n)$ and our numerical analysis brings evidence that each bound converges to 0 as $O\left(\frac{1}{\sqrt{n}}\right)$. In this section, by using repeatedly Stirling's formula, we prove this for a lower bound. The proof for an upper bound is still to be found, but we show the existence of upper bounds which are at least converging to 0 as $O\left(\frac{\ln(n)^{1.5}}{\sqrt{n}}\right)$ and even as $o\left(\sqrt{\frac{\ln^i(n)^3}{n}}\right)$, for any finite integer i , where $\ln^i(n)$ is recursively defined by $\ln^0(n) = n$ and $\forall j \in \mathbb{N}^*$, $\ln^j(n) = \ln^{j-1}(\ln(n))$.

4.1 Lower Bound

Let $r = r_{LB} = n_2 - \sqrt{n_2}$ (where $n_2 = \frac{n+1}{2}$); this is possible for an infinity of values of n (all those which can be expressed as twice a square minus 1: 7, 17, 31, 49, 71, ..., 19 999, ..., 1 999 999, ...). This restriction on the set of values of n which are considered makes the writing easier (which would otherwise call for the introduction of the integer parts). Let $n = 2 * s^2 - 1$, with s integer. Then, $r_{LB} = s(s - 1)$ and, from P7, the smallest $B^{k,l,r_{LB}}$ is obtained for $k = k_{LB} = s(s + 1) - 2$ and $l = l_{LB} = n_2 = s^2$. From P2, we deduce that all the $B^{k,l,r}$ (which exist) with $r > r_{LB}$ are larger than $B_{LB} = B^{k_{LB},l_{LB},r_{LB}}$. Finally, all the $B^{k,l,r}$ (which exist) with $0 \leq r < r_{LB}$ are strictly positive. Intuitively all the $B^{k,l,r}$ (which exist) constitute a kind of tetrahedron with an isosceles triangular base (for $r = 0$) and height $n_2 - 1$ (until $r = n_2 - 2$). Therefore, $\phi(n)$ which is equal to six times the sum of the cells of the tetrahedron (the $B^{k,l,r}$ which exist) is larger than six times the number of cells such that $r \geq r_{LB}$ multiplied by the smallest of these cells: B_{LB} . We also neglect all the values of the cells located on lower levels ($r < r_{LB}$). Let $\phi_m(n)$ denote the value of this lower bound. The number of cells such that $r \geq r_{LB}$ is the number of cells of the tetrahedron with isosceles triangular base and height $n_2 - 2 - r_{LB} + 1 = s - 1$. The number of cells for a tetrahedron of height h is $\frac{h(h+1)(h+2)}{6}$. When $h = s - 1$, the number of cells is therefore $\frac{(s-1)s(s+1)}{6}$. Furthermore, Stirling's formula (see appendix B) for B_{LB} implies $B_{LB} = O(s^{-4}) = O(n^{-2})$. Combining, we deduce: $\phi_m(n)$ is at least in $O(s^{-1}) = O\left(\frac{1}{\sqrt{n}}\right)$.

Note that this result only needs to consider one point (B_{LB}) in the tetrahedron. Besides, we have tried to consider more points in order to obtain the highest possible lower bound, but its order remains the same. So our conjecture seems to hold for the lower bound.

4.2 Upper Bound

This subsection first shows that the upper bound is at most in $O\left(\sqrt{\frac{\ln(n)^3}{n}}\right)$. This is obtained quite simply, using only two points of the tetrahedron (B_S and B_{I_1}). The subsection then tries to obtain the

lowest possible upper bound, making use of more points on the vertical edge of the tetrahedron. We show that the order of the upper bound is much lower, but $O\left(\frac{1}{\sqrt{n}}\right)$ still remains a conjecture.

Figure 12 shows all the points that were used in the tetrahedron.

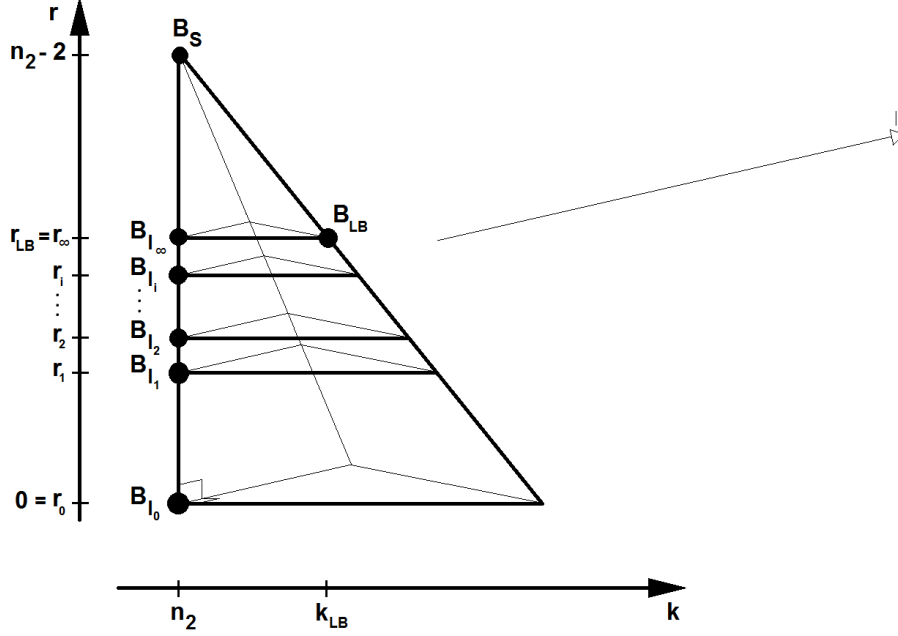


Figure 12: Representation of the tetrahedron containing all $B^{k,l,r}$ values that are added to compute ϕ , and the position of specific cells: B_{LB} , B_S , B_{I_0} , B_{I_1} , B_{I_2} , B_{I_i} and $B_{I_{\infty}}$.

4.2.1 A Coarse Upper Bound

From P5 and P2, we deduce that the largest value of the tetrahedron is obtained on the top: $B_S = B^{n_2, n_2, n_2 - 2}$. Stirling's formula (cf. appendix B) implies that this expression converges to 0 as $O(n^{-2})$. Let $r = r_1 = n_2 - \frac{3}{2}\sqrt{n_2 \ln(n)}$, where $n_2 = \frac{n+1}{2}$.

An upper bound of the top part of the tetrahedron (cells for which $r > r_1$) is obtained by replacing each value of these cells by the value of B_S . Since the height of this part is in $O\left(\sqrt{n \ln(n)}\right)$, we deduce that this part of the tetrahedron is majorized by an expression which converges to 0 as $O\left(\frac{\ln(n)^{1.5}}{\sqrt{n}}\right)$.

In the lower part of the tetrahedron ($r \leq r_1$), we also deduce from P5 and P2 that the largest value of a cell is obtained in $B_{I_1} = B^{n_2, n_2, r_1}$. Stirling's formula (see section B) implies that B_{I_1} converges much more rapidly than B_S to 0: precisely as $O(n^{-3.5})$. The height of this lower part of the tetrahedron is r_1 ; the length of its largest edge (for the base i.e. $r = 0$) is $n_2 - 1$. Therefore the number of cells of this part is lower than n^3 . Hence, this part of the tetrahedron is majorized by an expression which converges to 0 as $O\left(\frac{1}{\sqrt{n}}\right)$.

All together, we have obtained an upper bound of $\phi(n)$, denoted $\phi_{M_1}(n)$, verifying: $\phi_{M_1}(n) = O\left(\sqrt{\frac{\ln(n)^3}{n}}\right)$.

4.2.2 A Finer Upper Bound

To prove our conjecture, we would need to cut the tetrahedron into parts that are at most in $O\left(\frac{1}{\sqrt{n}}\right)$.

In the previous approach, the sum of the cells of the tetrahedron between the heights of B_{I_0} and B_{I_1} (lower part) is indeed at most in $O\left(\frac{1}{\sqrt{n}}\right)$, but the upper part was not.

Here, the upper part is again divided into pieces to obtain a finer upper bound.

Top part of the tetrahedron

As B_S is in $O(n^{-2})$, the top part till B_{I_∞} (which corresponds to a tetrahedron of height in $O(n^{0.5})$) is in $O\left(\frac{1}{\sqrt{n}}\right)$. Here, the order is exact, as all cells are in $O(n^{-2})$: the largest (B_S) as well as the smallest (B_{LB}) or also B_{I_∞} .

Layer B_{I_1} to B_{I_2} of the tetrahedron

Let $r_2 = n_2 - \frac{3}{2}\sqrt{n_2 \ln(\ln(n))}$. B_{I_2} is the point on the vertical edge of the tetrahedron for which $r = r_2$. Again, Stirling's formula (cf. appendix B) implies that the value in B_{I_2} is in $O(n^{-2} \ln(n)^{-1.5})$.

The volume of the tetrahedron layer between B_{I_1} and B_{I_2} is in $O((n \ln(n))^{1.5})$. And the highest value in this volume is at B_{I_2} . Hence, the sum of cells in this volume is at most in $O(n^{0.5})$.

Finally, only the tetrahedron part between B_{I_2} and B_{I_∞} remains to estimate. The corresponding volume is in $O((n \ln(\ln(n)))^{1.5})$. And the highest value in this volume is at B_{I_∞} , which is in $O(n^{-2})$. Hence, this part dominates the others, leading to a finer upper bound of $\phi(n)$, denoted $\phi_{M_2}(n)$, verifying: $\phi_{M_2}(n) = O\left(\sqrt{\frac{\ln(\ln(n))^3}{n}}\right)$.

Recursively refining the dominating layer up to $B_{I_i} - B_{I_\infty}$

Let i be an integer greater than 2 and B_{I_i} be on the vertical edge of the tetrahedron at $r = r_i$, with $r_i = n_2 - \frac{3}{2}\sqrt{n_2 \ln^i(n)}$, where $\ln^i(n)$ is recursively defined by $\ln^0(n) = n$ and $\forall j \in \mathbb{N}^*$, $\ln^j(n) = \ln^{j-1}(\ln(n))$.

All layers between B_{j-1} and B_j are at most in $O(n^{0.5})$, as the top part of the tetrahedron. As i is finite, the sum of all these $i + 1$ volumes is also at most in $O(n^{0.5})$.

The dominating part corresponds to the layer between B_{I_i} and B_{I_∞} . The corresponding volume is in $O((n \ln^i(n))^{1.5})$. And the highest value in this volume is again at B_{I_∞} , which still is in $O(n^{-2})$.

This recursively leads to a finer upper bound of $\phi(n)$, denoted $\phi_{M_i}(n)$, verifying: $\phi_{M_i}(n) = O\left(\sqrt{\frac{\ln^i(n)^3}{n}}\right)$.

As this is true also at $i + 1$, we can also write $\phi(n) = o(\phi_{M_i}(n))$.

Upper bound summary

This subsection has proven that for any finite integer i , $\phi(n)$ is dominated by $\sqrt{\frac{\ln^i(n)^3}{n}}$.

Note that, from numerical results, we believe that a closer upper bound converging even faster towards 0 (in $O\left(\frac{1}{\sqrt{n}}\right)$) exists. But we leave that part as a conjecture²².

5 Concluding Remarks

In this paper, we have focused our attention on the case of three equipopulated districts. We have shown that the *IAC* probability of a divided verdict tends to zero, at least as $O\left(\frac{\ln(n)^{1.5}}{\sqrt{n}}\right)$ and we conjecture that it should be $O\left(\frac{1}{\sqrt{n}}\right)$. It is of course of interest to know if this inverse square root result is entirely driven by our stylistic assumptions. We have not been able to derive closed form formulas for the general equipopulated case, but we have run simulations for several values of K , the number of states, ranging from 3 to 101. If we denote $\phi(K, n)$ the *IAC* probability of an election inversion when there are K states and n voters per state, the graph of $\sqrt{n}\phi(K, n)$ resulting from these simulations is depicted in figure 13 below for a range of values of n .

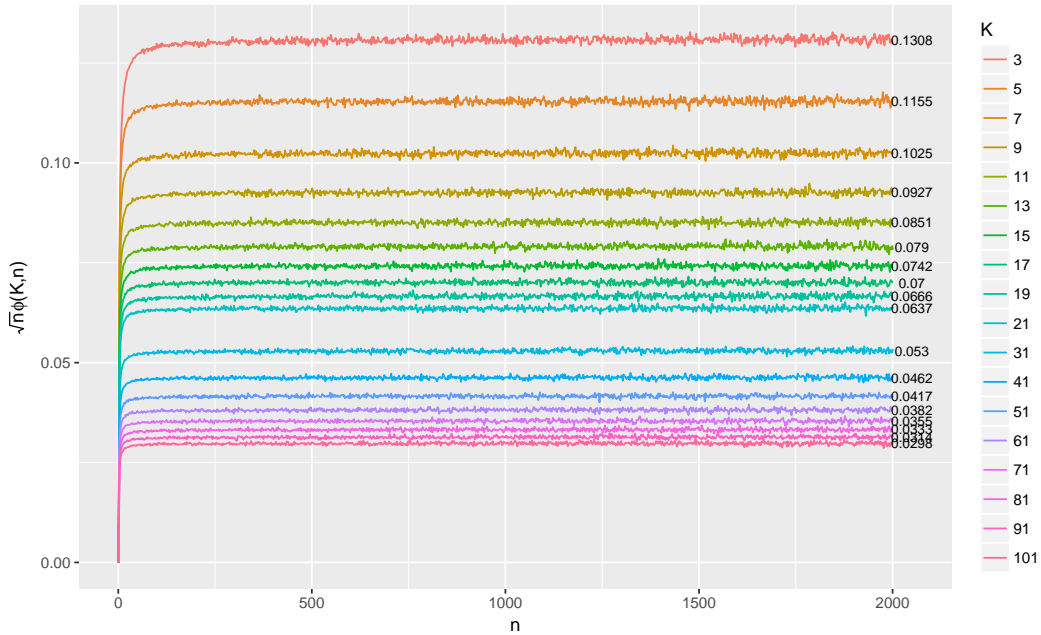


Figure 13: Simulated Graph of $\sqrt{n}\phi(K, n)$.

Note first that the simulations confirm the result established in this paper that is the convergence of $\sqrt{n}\phi(3, n)$ towards a value between 0.125 and 0.150. Second, this sample of values of K suggests that

²²Indeed the result we have obtained in this subsection is not sufficient to get rid of the factor $\ln^i(n)^{1.5}$. Proving the conjecture would require to study analytically the sum $\phi(n)$ or, which might slightly be easier, the sum ϕ_{maj} , see (6), at least for values of r between r_i and r_∞ . But this difficult task still remains to be done.

the inverse square root speed of convergence property, that is the convergence of $\sqrt{n}\phi(K, n)$ towards a constant $\theta(K)$, is not specific to the three states case. But computing the constant $\theta(K)$ is pretty challenging: simulations suggest that $\theta(51)$ is around 0.0417. Simulations also suggest that $\theta(K)$ is decreasing with respect to K . Of course, this is a first step and some further mathematical and numerical analysis is needed to reach a deeper understanding of this question.

References

- [1] Banzhaf, J.F. (1965) "Weighted voting does not work: a mathematical analysis", *Rutgers Law Review*, 19, 317-343.
- [2] Banzhaf, J.F. (1966) "Multi-member electoral districts: do they violate the one man, one vote principle", *Yale Law Journal*, 75, 1309-1338.
- [3] Chamberlain, G. and M. Rothschild (1981) "A Note on the Probability of Casting a Decisive Vote", *Journal of Economic Theory*, 25, 152-162.
- [4] Feix, M.R., Lepelley, D., Merlin, V. and J.L. Rouet (2004) "The probability of conflicts in a U.S. presidential type election", *Economic Theory*, 23, 227-257.
- [5] Gehrlein, W.V. and D. Lepelley (2011) *Voting Paradoxes and Group Coherence*, Springer.
- [6] Fishburn, P.C. and W.V. Gehrlein (1976) "Borda's Rule, Positional Voting, and Condorcet's Simple Majority Principle", *Public Choice*, 28, 79-88.
- [7] Good, I.J. and L.S. Mayer (1975) "Estimating the Efficacy of a Vote", *Behavioral Science*, 20, 25-33.
- [8] Hinich, M.J. Mickelsen, R. and P.C. Ordeshook (1972) "The Electoral College Versus a Direct Vote: Policy Bias, Reversals, and Indeterminate Outcomes", *Journal of Mathematical Sociology*, 4, 3-35.
- [9] Kaniowski, S. and A. Zaihraev (2017) "The Probability of Majority Inversion in a Two-Stage Voting System with Three States, Austrian Institute of Economic Research, Mimeo.
- [10] Kikuchi, K. (2017) "The Likelihood of Majority Inversion in an Indirect Voting System", Waseda University, Mimeo.
- [11] Kikuchi, K. (2018) "A Note on Election Inversion", Mimeo, Private Correspondence.

- [12] Kuga, K. and H. Nagatani (1974) “Voter Antagonism and the Paradox of Voting”, *Econometrica*, 42, 1045-1067.
- [13] Le Breton, M. and D. Lepelley (2014) "Une Analyse de la Loi Electorale du 29 Juin 1820", *Revue Économique*, 65, 469–518.
- [14] Le Breton, M., Lepelley, D. and H. Smaoui (2016) “Correlation, Partitioning and the Probability of Casting a Decisive Vote under the Majority Rule”, *Journal of Mathematical Economics*, 64, 11–22.
- [15] Lepelley, D., Merlin, V. and J.L. Rouet (2011) “Three Ways to Compute accurately the probability of the Referendum paradox”, *Mathematical Social Sciences*, 23, 227-257.
- [16] May, K. (1948) “Probability of Certain Election Results”, *American Mathematical Monthly*, 55, 203-209.
- [17] Miller, N.R. (2012a) “Election Inversions by the U.S. Electoral College”, Chapter 4 in *Electoral Systems*, Studies in Social Choice and Welfare, Felsenthal, D.DS. and M. Machover (Eds), Springer-Verlag, Berlin Heidelberg.
- [18] Miller, N.R. (2012b) “Why the Electoral College is Good for Political Science (and Public Choice)”, *Public Choice*, 150, 1–25.
- [19] Nurmi, H. (1999) *Voting paradoxes and How to deal with Them*, Springer-Verlag, Berlin.
- [20] Owen, G. (1975) Evaluation of a Presidential Election Game, *American Political Science Review*, 69, 947-953.
- [21] Shapley, L.S. and M. Shubik (1954) “A method for evaluating the distribution of power in a committee system”, *American Political Science Review*, 48, 787-792.
- [22] Straffin P.D. (1988) “The Shapley-Shubik and Banzhaf Power Indices as Probabilities”, in A.E. Roth (eds.) *The Shapley Value: Essays in Honor of Lloyd S. Shapley*, Cambridge University Press
- [23] Tuftes, E.R. (1973) “The Relationship between Seats and Votes in Two-Party Systems”, *American Journal of Political Science*, 67, 540-554.

A Proofs

A.1 P1. $B^{k,l,r} = B^{l,k,r}$

Follows trivially from commuting addition and multiplication:

$$\begin{aligned} B^{l,k,r} &= \binom{n}{l} \binom{n}{k} \binom{n}{r} \frac{(l+k+r)!(3n-l-k-r)!}{(3n+1)!} \\ &= \binom{n}{k} \binom{n}{l} \binom{n}{r} \frac{(k+l+r)!(3n-k-l-r)!}{(3n+1)!} = B^{k,l,r} \end{aligned}$$

A.2 P2. $B^{k,l,r} > B^{k,l,r-1}$ (for values k, l, r and $r-1$ which are feasible)

$$\begin{aligned} \frac{B^{k,l,r}}{B^{k,l,r-1}} &= \frac{\binom{n}{r} (k+l+r)!(3n-k-l-r)!}{\binom{n}{r-1} (k+l+r-1)!(3n-k-l-r+1)!} \\ &= \frac{(r-1)!(n-r+1)!}{r!(n-r)!} \frac{(k+l+r)!(3n-k-l-r)!}{(k+l+r-1)!(3n-k-l-r+1)!} \\ &= \frac{n-r+1}{r} \frac{k+l+r}{3n-k-l-r+1} \end{aligned}$$

Since all the numbers are positive, we deduce:

$$B^{k,l,r} > B^{k,l,r-1} \tag{7}$$

$$\begin{aligned} &\Leftrightarrow \frac{(n-r+1)(k+l+r)}{r(3n-k-l-r+1)} > 1 \\ &\Leftrightarrow (n-r+1)(k+l+r) > r(3n-k-l-r+1) \\ &\Leftrightarrow (n+1)(k+l) > r(3n-k-l+1-n-1+k+l) \\ &\Leftrightarrow \frac{(n+1)(k+l)}{2n} > r \end{aligned} \tag{8}$$

Further, $k \geq n_2$

and $l \geq n_2$

with $n_2 = \frac{n+1}{2}$

which implies $k+l \geq n+1$

$$\text{i.e. } \frac{(n+1)(k+l)}{2n} \geq \frac{(n+1)^2}{2n} = n_2 + \frac{1}{2} + \frac{1}{2n} > n_2 - 2 \tag{9}$$

$$\text{Finally, } r \leq \frac{3n-1}{2} - k - l$$

$$\begin{aligned}
& k \geq n_2 \\
& \text{and } l \geq n_2 \\
& \text{implies } r \leq \frac{3n-1-2n-2}{2} = n_2 - 2
\end{aligned} \tag{10}$$

Combining (10) and (9) implies (8) and then (7).

A.3 P3. $B^{k,l,r} > B^{k+1,l,r}$ (for values of k, l, r and $k+1$ which are feasible)

$$\begin{aligned}
\frac{B^{k,l,r}}{B^{k+1,l,r}} &= \frac{\binom{n}{k} (k+l+r)!(3n-k-l-r)!}{\binom{n}{k+1} (k+1+l+r)!(3n-k-1-l-r)!} \\
&= \frac{(k+1)!(n-k-1)!}{k!(n-k)!} \cdot \frac{(k+l+r)!(3n-k-l-r)!}{(k+1+l+r)!(3n-k-1-l-r)!} \\
&= \frac{k+1}{n-k} \cdot \frac{3n-k-l-r}{k+1+l+r}
\end{aligned}$$

Again, since all the numbers are positive, this implies::

$$\begin{aligned}
& B^{k,l,r} > B^{k+1,l,r} \tag{11} \\
& \Leftrightarrow \frac{k+1}{n-k} \cdot \frac{3n-k-l-r}{k+1+l+r} > 1 \\
& \Leftrightarrow (k+1)(3n-k-l-r) > (n-k)(k+1+l+r) \\
& \Leftrightarrow k(3n-l-r-1+1+l+r-n) > n(1+l+r) - 3n+l+r \\
& \Leftrightarrow k > \frac{(n+1)(l+r) - 2n}{2n} \tag{12}
\end{aligned}$$

$$\text{Further } k \geq n_2 \tag{13}$$

$$\begin{aligned}
& \text{and } l+r \leq \frac{3n-1}{2} - k \\
& \text{implies } l+r \leq n-1 \\
& \text{i.e. } \frac{(n+1)(l+r) - 2n}{2n} \leq \frac{(n-1)^2}{2n} = n_2 - \frac{3}{2} - \frac{1}{2n} < n_2 \tag{14}
\end{aligned}$$

Combining (14) and (13) implies(12) and then (11).

A.4 P4. $B^{k,l,r} > B^{k,l+1,r}$ (for values of k, l, r and $l+1$ which are feasible)

The proof is a trivial implication of P1 and P3: $B^{k,l,r} = B^{l,k,r} > B^{l+1,k,r} = B^{k,l+1,r}$.

A.5 P5. For each fixed r , $B^{k,l,r}$ is maximized when $k = l = n_2 (= \frac{n+1}{2})$

It follows trivially from P3 with $k \geq n_2$ and P4 with $l \geq n_2$.

A.6 P6. $\forall l \geq k, B^{k,l,r} > B^{k-1,l+1,r}$ (for values of $k, k-1, l, l+1$ and r which are feasible)

From the beginning of the proof of P3 and P1, we deduce:

$$\begin{aligned} \frac{B^{k+1,l,r}}{B^{k,l+1,r}} &= \frac{B^{k,l,r}}{B^{k,l+1,r}} \times \frac{1}{\frac{B^{k,l,r}}{B^{k+1,l,r}}} \\ &= \left(\frac{l+1}{n-l} \times \frac{3n-k-l-r}{k+1+l+r} \right) \left(\frac{1}{\frac{k+1}{n-k} \times \frac{3n-k-l-r}{k+1+l+r}} \right) \\ &= \frac{l+1}{n-l} \times \frac{n-k}{k+1} \end{aligned}$$

And since all numbers are positive

$$\begin{aligned} B^{k,l,r} &> B^{k-1,l+1,r} & (15) \\ \Leftrightarrow \frac{l+1}{n-l} \cdot \frac{n-k+1}{k} &> 1 \\ \Leftrightarrow \frac{k+j+1}{n-k-j} \cdot \frac{n-k+1}{k} &> 1 \\ \Leftrightarrow (l+1)(n+1) - k - kl &> nk - kl \\ \Leftrightarrow (l+1)(n+1) &> k(n+1) \\ \Leftrightarrow (l+1) &> k & (16) \end{aligned}$$

But since(16) holds true for $l \geq k$, we deduce(15).

Remark: if $l < k$, we obtain a symmetric result via P1.

A.7 P7. For each fixed r , $B^{k,l,r}$ is minimized when $k = n - 1 - r$ and $l = n_2$

From P3 and P4, we deduce that the minimum is obtained on the base of the “isosceles triangle defined by $B^{k,l,r}$ entries such that $k+l = \frac{3n-1}{2} - r$ ”. From P6 and P1, the minimum is reached when k or l is equal to n_2 (the other being then equal to $n - 1 - r$).

B Taylor Expansions Using Stirling’s Formula

This section explains in more details how the different asymptotic behaviors are obtained for specific $B^{k,l,r}$ used in the paper and represented on Figure 14. It all starts with Stirling’s formula (and series) as $B^{k,l,r}$ is composed of products and divisions of different factorials.

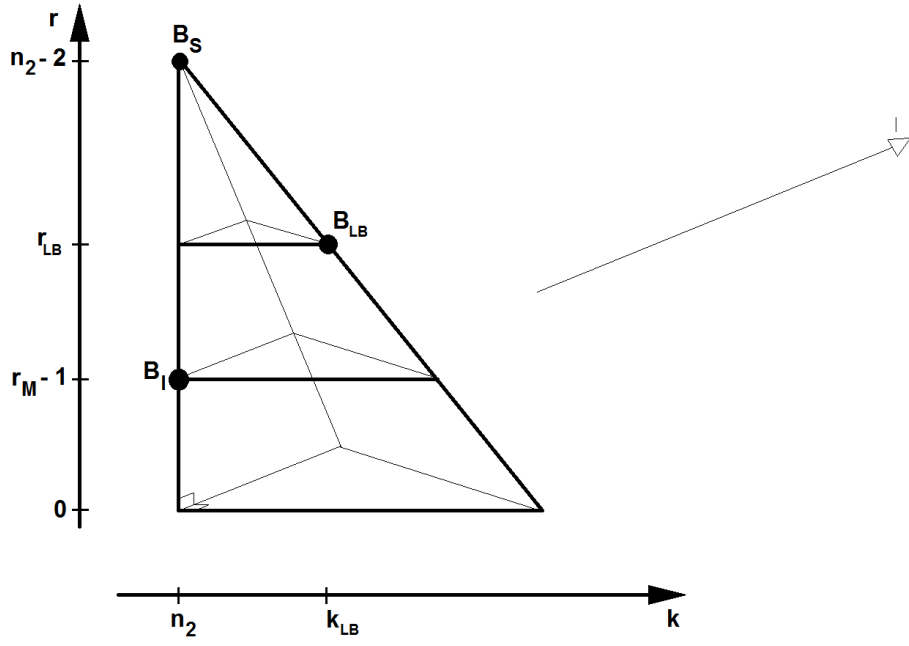


Figure 14: Representation of the tetrahedron containing all $B^{k,l,r}$ values that are added to compute ϕ , and the position of specific cells: B_{LB} , B_S and B_I .

B.1 Approximations of $n!$ or $\ln(n!)$

Stirling's formula gives an asymptotic approximation of factorial as:

$$n! \sim \sqrt{2\pi n} \left(\frac{n}{e}\right)^n.$$

This approximation is in $o(1)$ (in fact $O(n^{-1})$) and is used below in Tables 3, 4 and 5.

In fact, with Taylor expansions, Stirling's formula leads to Stirling series, which are used in (3) to compute an accurate approximation of $\ln\Gamma(n)$.

For instance, $\ln\Gamma(n+1) =$

$$\ln(n!) \sim n \ln(n) - n + \frac{1}{2} \ln(2\pi n) + \frac{1}{12n} - \frac{1}{360n^3} + \frac{1}{1260n^5} - \frac{1}{1680n^7} + \frac{1}{1188n^9} + \dots$$

B.2 Approximations for $B^{k,l,r}$ values in B_S , B_I and B_{LB}

Using this approximation in $\ln(B^{k,l,r})$ leads to approximations for values in B_S , B_I and B_{LB} (their position in the tetrahedron are shown in figure 14), with:

$$\ln(B^{k,l,r}) = 3 \ln\Gamma(n+1) \tag{17}$$

$$+ \ln\Gamma(k+l+r+1) \tag{18}$$

$$+ \ln\Gamma(3n-k-l-r+1) \tag{19}$$

$$- \ln\Gamma(k+1) \quad (20)$$

$$- \ln\Gamma(n-k+1) \quad (21)$$

$$- \ln\Gamma(l+1) \quad (22)$$

$$- \ln\Gamma(n-l+1) \quad (23)$$

$$- \ln\Gamma(r+1) \quad (24)$$

$$- \ln\Gamma(n-r+1) \quad (25)$$

$$- \ln\Gamma(3n+2). \quad (26)$$

The approximations used for the different elements of this sum can be found in Table 3, Table 4 and Table 5.

$\ln\Gamma(i_n) =$	$\alpha_{i_n} n \ln(n)$	$+\beta_{i_n} n$	$+\gamma_{i_n} \ln(n)$	$+\delta_{i_n} + O(n^{-1})$
i_n	α_{i_n}	β_{i_n}	γ_{i_n}	δ_{i_n}
$\frac{n-1}{2}$	$\frac{1}{2}$	$-\frac{1+\ln(2)}{2}$	-1	$\frac{1}{2}\ln(8\pi)$
$\frac{n+1}{2}$	$\frac{1}{2}$	$-\frac{1+\ln(2)}{2}$	0	$\frac{1}{2}\ln(2\pi)$
$\frac{n+3}{2}$	$\frac{1}{2}$	$-\frac{1+\ln(2)}{2}$	1	$\frac{1}{2}\ln\left(\frac{\pi}{2}\right)$
$\frac{n+5}{2}$	$\frac{1}{2}$	$-\frac{1+\ln(2)}{2}$	2	$\frac{1}{2}\ln\left(\frac{\pi}{8}\right)$
$n+1$	1	-1	$\frac{1}{2}$	$\frac{1}{2}\ln(2\pi)$
$\frac{3n+1}{2}$	$\frac{3}{2}$	$-\frac{3}{2}\left(1-\ln\left(\frac{3}{2}\right)\right)$	0	$\frac{1}{2}\ln(2\pi)$
$\frac{3n+3}{2}$	$\frac{3}{2}$	$-\frac{3}{2}\left(1-\ln\left(\frac{3}{2}\right)\right)$	1	$\frac{1}{2}\ln\left(\frac{9\pi}{2}\right)$
$3n+2$	3	$-3+3\ln(3)$	$\frac{3}{2}$	$\frac{1}{2}(3\ln(3)+\ln(2\pi))$

Table 3: Approximations of $\ln\Gamma(i)$ for different integers i (in ascending order), using Stirling's formula: $\ln\Gamma(i_n) = \alpha_{i_n} n \ln(n) + \beta_{i_n} n + \gamma_{i_n} \ln(n) + \delta_{i_n} + O(n^{-1})$.

The following subsections, are organized to give first common approximations of some parts of $\ln(B^{k,l,r})$, either to any points of the tetrahedron: (17) and (26), or to the points of one of its face (l minimal): (22) and (23), or even to the points of its vertical edge (k also minimal): (20), (21). Then the specific approximations of remaining parts of $\ln(B^{k,l,r})$ are given for each point (B_S , B_{LB} and B_I), leading to final approximation for each of the three specific points on the tetrahedron.

For each of the three considered points in the tetrahedron, Table 3 is used. This sole table is sufficient for B_S . For B_{LB} , Table 4 is also required. And for B_I , the second required table is Table 5.

B.2.1 Common approximations for B_S , B_I and B_{LB}

Parts (17) and (26) are common to all $\ln(B^{k,l,r})$, leading to the following approximation:

$$3 \ln \Gamma(n+1) - \ln \Gamma(3n+2) = -3 \ln(3)n - \frac{3}{2} \ln(3) + \ln(2\pi) + O(n^{-1}).$$

B.2.2 Approximations for B_{LB} which are similar to common approximations for B_S and B_I

Tetrahedron face $l = \frac{n+1}{2}$

For all points on the face of the tetrahedron presented in figure 14 (i.e. $l = n_2$, with $n_2 = \frac{n+1}{2}$), parts (22) and (23) can be simplified into:

$$\begin{aligned} (22): \quad \ln \Gamma(l+1) &= \ln \Gamma\left(\frac{n+3}{2}\right) \\ (23): \quad \ln \Gamma(n-l+1) &= \ln \Gamma\left(\frac{n+1}{2}\right). \end{aligned}$$

This finally leads to the following approximation, when $l = n_2$ as for B_{LB} :

$$\begin{aligned} -\ln \Gamma(l+1) - \ln \Gamma(n-l+1) &= \\ &= -n \ln(n) + (1 + \ln(2))n - \ln(n) - \ln(\pi) + O(n^{-1}). \end{aligned}$$

Tetrahedron edge $k = l = \frac{n+1}{2}$

For all points on the vertical edge of the tetrahedron (i.e. $k = l = n_2$, with $n_2 = \frac{n+1}{2}$), parts (20) and (21) can similarly be simplified by symmetry ($k = l$): (20) is equivalent to (22) and (21) is equivalent to (23).

This finally leads to the following approximation, when $k = l = n_2$ as for B_S and B_I :

$$\begin{aligned} -\ln \Gamma(k+1) - \ln \Gamma(n-k+1) - \ln \Gamma(l+1) - \ln \Gamma(n-l+1) &= \\ &= -2n \ln(n) + 2(1 + \ln(2))n - 2 \ln(n) - 2 \ln(\pi) + O(n^{-1}). \end{aligned}$$

B.2.3 Final approximation for B_S

The peak of the tetrahedron, B_S , is located at $k = l = n_2$ and $r = n_2 - 2$. So, the four last remaining parts of $\ln(B^{k,l,r})$ to approximate for B_S can be simplified into:

$$(18): \quad \ln \Gamma(k+l+r+1) = \ln \Gamma\left(\frac{3n+1}{2}\right)$$

$$\begin{aligned}
(19): \quad \ln\Gamma(3n - k - l - r + 1) &= \ln\Gamma\left(\frac{3n+3}{2}\right) \\
(24): \quad \ln\Gamma(r + 1) &= \ln\Gamma\left(\frac{n-1}{2}\right) \\
(25): \quad \ln\Gamma(n - r + 1) &= \ln\Gamma\left(\frac{n+5}{2}\right).
\end{aligned}$$

This leads to the following approximation, when $k = l = n_2$ and $r = n_2 - 2$ (B_S):

$$\begin{aligned}
\ln\Gamma(k + l + r + 1) + \ln\Gamma(3n - k - l - r + 1) - \ln\Gamma(r + 1) - \ln\Gamma(n - r + 1) = \\
2n \ln(n) - (2(1 + \ln(2)) - 3 \ln(3))n + \ln(3) + O(n^{-1}).
\end{aligned}$$

Summing all parts for the approximation of $\ln(B^{k,l,r})$ value in B_S , leads to:

$$\ln(B^{n_2, n_2, n_2-2}) = -2 \ln(n) + \ln\left(\frac{2}{\pi\sqrt{3}}\right) + O(n^{-1}).$$

Finally, in B_S , B^{n_2, n_2, n_2-2} reads:

$$B^{n_2, n_2, n_2-2} = \frac{2}{\pi\sqrt{3}n^2} + O(n^{-3}) = O(n^{-2}). \quad (27)$$

B.2.4 Final approximation for B_{LB}

B_{LB} , is located at $k = n_2 + \sqrt{n_2} - 2$, $l = n_2$ and $r = n_2 - \sqrt{n_2}$. So, the six remaining parts of $\ln(B^{k,l,r})$ to approximate for B_{LB} can be simplified into:

$$\begin{aligned}
(20): \quad \ln\Gamma(k + 1) &= \ln\Gamma\left(\frac{n-1}{2} + \sqrt{\frac{n+1}{2}}\right) \\
(22): \quad \ln\Gamma(n - k + 1) &= \ln\Gamma\left(\frac{n+5}{2} - \sqrt{\frac{n+1}{2}}\right) \\
(18): \quad \ln\Gamma(k + l + r + 1) &= \ln\Gamma\left(\frac{3n+1}{2}\right) \\
(19): \quad \ln\Gamma(3n - k - l - r + 1) &= \ln\Gamma\left(\frac{3n+3}{2}\right) \\
(24): \quad \ln\Gamma(r + 1) &= \ln\Gamma\left(\frac{n+3}{2} - \sqrt{\frac{n+1}{2}}\right) \\
(25): \quad \ln\Gamma(n - r + 1) &= \ln\Gamma\left(\frac{n+1}{2} + \sqrt{\frac{n+1}{2}}\right).
\end{aligned}$$

The approximations for the two middle parts can be found in Table 3. As for the two first and two last parts, their approximations can be found in Table 4.

Looking for the approximations of the four values in Table 4 leads to the following approximation, when $k = n_2 + \sqrt{n_2} - 2$, $l = n_2$ and $r = n_2 - \sqrt{n_2}$ (B_{LB}):

i_n	α_{i_n}	β_{i_n}	γ_{i_n}	δ_{i_n}	ε_{i_n}	ζ_{i_n}
$\frac{n+3}{2} - \sqrt{\frac{n+1}{2}}$	$\frac{1}{2}$	$-\frac{1+\ln(2)}{2}$	$-\frac{1}{\sqrt{2}}$	$\frac{\ln(2)}{\sqrt{2}}$	1	$\frac{1+\ln(\frac{\pi}{2})}{2}$
$\frac{n+5}{2} - \sqrt{\frac{n+1}{2}}$	$\frac{1}{2}$	$-\frac{1+\ln(2)}{2}$	$-\frac{1}{\sqrt{2}}$	$\frac{\ln(2)}{\sqrt{2}}$	2	$\frac{1+\ln(\frac{\pi}{8})}{2}$
$\frac{n-1}{2} + \sqrt{\frac{n+1}{2}}$	$\frac{1}{2}$	$-\frac{1+\ln(2)}{2}$	$\frac{1}{\sqrt{2}}$	$-\frac{\ln(2)}{\sqrt{2}}$	-1	$\frac{1+\ln(\frac{\pi}{2})}{2}$
$\frac{n+1}{2} + \sqrt{\frac{n+1}{2}}$	$\frac{1}{2}$	$-\frac{1+\ln(2)}{2}$	$\frac{1}{\sqrt{2}}$	$-\frac{\ln(2)}{\sqrt{2}}$	0	$\frac{1+\ln(2\pi)}{2}$

Table 4: Approximations of $\ln\Gamma(i)$ for different integers i (in ascending order), using Stirling's formula: $\ln\Gamma(i_n) = \alpha_{i_n}n\ln(n) + \beta_{i_n}n + \gamma_{i_n}\sqrt{n}\ln(n) + \delta_{i_n}\sqrt{n} + \varepsilon_{i_n}\ln(n) + \zeta_{i_n} + O\left(\frac{1}{\sqrt{n}}\right)$.

$$-\ln\Gamma(k+1) - \ln\Gamma(n-k+1) + \ln\Gamma(k+l+r+1) + \ln\Gamma(3n-k-l-r+1) - \ln\Gamma(r+1) - \ln\Gamma(n-r+1) = n\ln(n) + (3\ln(3) - (1+\ln(2)))n - \ln(n) - \left(2 + \ln\left(\frac{\pi}{3}\right)\right) + O\left(n^{-0.5}\right).$$

Summing all parts for the approximation of $\ln(B^{k,l,r})$ value in B_{LB} , leads to:

$$\ln(B^{n_2+\sqrt{n_2}-2, n_2, n_2-\sqrt{n_2}}) = -2\ln(n) - 2 + \ln\left(\frac{2}{\pi\sqrt{3}}\right) + O\left(n^{-0.5}\right).$$

Finally, in B_{LB} , $B^{n_2+\sqrt{n_2}-2, n_2, n_2-\sqrt{n_2}}$ reads:

$$B^{n_2+\sqrt{n_2}-2, n_2, n_2-\sqrt{n_2}} = \frac{2}{\pi\sqrt{3}n^2e^2} + O\left(n^{-2.5}\right) = O\left(n^{-2}\right). \quad (28)$$

Note that the value in B_{LB} is of the same order as in B_S . In fact, when n tends to infinity, the relation between the two tends to e^{-2} .

B.2.5 Final approximation for B_I

Looking at a range of heights on the vertical edge of the tetrahedron to find B_I

Point B_I is located on the vertical edge of the tetrahedron ($k = l = n_2$) at height $r = r_M - 1$. Here, we are looking for a point where the sum of all cells at this height and below is converging towards 0 at least in $O\left(n^{-0.5}\right)$. For this aim, we chose $r_M = n_2 - \sqrt{n_2}f(n)$, i.e. height $r = \frac{n-1}{2} - \sqrt{n_2}f(n)$, with f a positive function which does not increase too much: $\lim_{n \rightarrow +\infty} r \geq 0$, i.e. r has to remain positive (at

least for large enough n). So f is at most equivalent to $\sqrt{n_2} - 1 - o(\sqrt{n})$, when n tends to infinity. In fact, when using Taylor expansions, there is a difference between $f = O(\sqrt{n})$, $f = o(\sqrt{n})$ and $\exists x < 0.5/f = O(n^x)$.

So this subsection is valid only for:

$$f \text{ is a positive function such that } \exists x < 0.5 \text{ with } f = O(n^x). \quad (29)$$

Under this condition, $\lim_{n \rightarrow +\infty} r_M = \infty$. So, every asymptotic result that hold in this section with r_M that might not be integer still hold if we consider only the integer part of r_M , the rest being negligible (at least for large enough values of n).

Exemplifying the approximations in this subsection with function f

For instance, to better understand the approximations that use Taylor expansions, $\ln(n - \sqrt{n}f(n))$ would give:

$$\ln(n - \sqrt{n}f(n)) = \ln(n) + \ln\left(1 - \frac{f(n)}{\sqrt{n}}\right).$$

As (29) means that $\frac{f(n)}{\sqrt{n}} = o(1)$, it is possible to use the Taylor expansion of $\ln(1 + u)$ when u is close to 0:

$$\ln(1 + u) = u - \frac{1}{2}u^2 + \frac{1}{3}u^3 - \frac{1}{4}u^4 + \dots$$

Hence, $\ln((n - \sqrt{n}f(n))!)$ would give:

$$\begin{aligned} \ln((n - \sqrt{n}f(n))!) &= \frac{1}{2} \ln(2\pi) - (n - \sqrt{n}f(n)) \\ &\quad + \left(n - \sqrt{n}f(n) + \frac{1}{2}\right) \ln(n - \sqrt{n}f(n)) + o(1) \\ &= \frac{1}{2} \ln(2\pi) - n + \sqrt{n}f(n) + o(1) \\ &\quad + \left(n - \sqrt{n}f(n) + \frac{1}{2}\right) \left(\ln(n) + \frac{f(n)}{n^{0.5}} - \frac{1}{2} \frac{f(n)^2}{n} + \frac{1}{3} \frac{f(n)^3}{n^{1.5}} - \frac{1}{4} \frac{f(n)^4}{n^2} + \dots\right) \\ &= \frac{1}{2} \ln(2\pi) - n + \sqrt{n}f(n) + o(1) \\ &\quad + n \ln(n) + f(n)n^{0.5} - \frac{1}{2}f(n)^2 + \frac{1}{3} \frac{f(n)^3}{n^{0.5}} - \frac{1}{4} \frac{f(n)^4}{n} + \dots \\ &\quad - \sqrt{n} \ln(n)f(n) - f(n)^2 + \frac{1}{2} \frac{f(n)^3}{n^{0.5}} - \frac{1}{3} \frac{f(n)^4}{n} + \frac{1}{4} \frac{f(n)^5}{n^{1.5}} - \dots \\ &\quad + \frac{\ln(n)}{2} + \frac{f(n)}{2n^{0.5}} - \frac{f(n)^2}{4n} + \frac{f(n)^3}{6n^{1.5}} - \frac{f(n)^4}{8n^2} + \dots \\ &= \frac{1}{2} \ln(2\pi) - n + \sqrt{n}f(n) + o(1) \\ &\quad + n \ln(n) + f(n)n^{0.5} - \frac{f(n)^2}{2} + \frac{f(n)^3}{3n^{0.5}} - \frac{f(n)^4}{4n} + \dots \end{aligned}$$

$$\begin{aligned}
& \text{until } \frac{(-1)^p f(n)^p}{pn^{\frac{p}{2}-1}} = o(1), \text{ and } p \text{ finite from (29)} \\
& -\sqrt{n}\ln(n)f(n) - f(n)^2 + \frac{f(n)^3}{2n^{0.5}} - \frac{f(n)^4}{3n} + \frac{f(n)^5}{4n^{1.5}} - \dots \\
& \text{until } \frac{(-1)^q f(n)^{q+1}}{qn^{\frac{q-1}{2}}} = o(1), \text{ and } q = p - 1 \\
& + \frac{\ln(n)}{2} + o(1), \text{ because } \frac{f(n)}{2n^{0.5}} = o(1) \text{ from (29)}.
\end{aligned}$$

Note that p is finite, as (29) implies $\frac{f(n)}{\sqrt{n}} = O\left(\frac{1}{n^{0.5-x}}\right)$, with $0.5 - x > 0$. So p is such that $(p+1)(0.5-x) > 1$, i.e. $p = \lfloor \frac{1}{0.5-x} \rfloor$. For instance, if $f(n) = n^{\frac{1}{8}}$ (i.e. $x = 0.125$), then $p = 2$ is sufficient (and $q = 1$).

Finally, if we stop at $p = 2$, then, for all f such that $f = o\left(n^{\frac{1}{6}}\right)$, we obtain:

$$\begin{aligned}
\ln((n - \sqrt{n}f(n))!) &= \frac{1}{2}\ln(2\pi) - n + \sqrt{n}f(n) + o(1) \\
&+ n\ln(n) + f(n)n^{0.5} - \frac{f(n)^2}{2} + o(1) \\
&- \sqrt{n}\ln(n)f(n) - f(n)^2 + o(1) \\
&+ \frac{\ln(n)}{2} + o(1) \\
&= n\ln(n) - n - \sqrt{n}\ln(n)f(n) + 2\sqrt{n}f(n) + \frac{\ln(n)}{2} - \frac{3f(n)^2}{2} + \frac{\ln(2\pi)}{2} + o(1)
\end{aligned}$$

Specific approximations for B_l involving f

Let $\ln(B_R^f) = \ln(B^{n_2, n_2, n_2 - \sqrt{n_2}f(n) - 1})$. The four last remaining parts of $\ln(B_R^f)$ to approximate for B_S can be simplified into:

$$(18): \quad \ln\Gamma(k+l+r+1) = \ln\Gamma\left(\frac{3n+3}{2} - \sqrt{\frac{n+1}{2}}f(n)\right)$$

$$(19): \quad \ln\Gamma(3n-k-l-r+1) = \ln\Gamma\left(\frac{3n+1}{2} + \sqrt{\frac{n+1}{2}}f(n)\right)$$

$$(24): \quad \ln\Gamma(r+1) = \ln\Gamma\left(\frac{n+1}{2} - \sqrt{\frac{n+1}{2}}f(n)\right)$$

$$(25): \quad \ln\Gamma(n-r+1) = \ln\Gamma\left(\frac{n+3}{2} + \sqrt{\frac{n+1}{2}}f(n)\right).$$

Table 5 gives the corresponding approximations. Note that the approximations have terms in $n\ln(n)$ (highest order), $\sqrt{n}\ln(n)f(n)$ and $\ln(n)$, have a constant, and have a series of terms in $n^{1-\frac{p}{2}}f(n)^p$, $p \in \mathbb{N}$.

As we want an approximation up to $o(1)$, we do not need all terms of the series. The number of terms depends on f . For instance, should f be a decreasing function, then only one (n , if $f = o\left(\frac{1}{\sqrt{n}}\right)$) or two terms (n and $\sqrt{n}f(n)$) of the series are enough. If f is strongly decreasing: $f = o\left(\frac{1}{\sqrt{n}\ln(n)}\right)$, then even the term in $\sqrt{n}\ln(n)f(n)$ can be skipped. Now, if $\lim_{n \rightarrow +\infty} f(n)$ is a constant, then we may stop at the third term (in $f(n)^2$). Similarly, if f is an increasing function, we may need to add more terms. And the more increasing the function is, the more terms need to be added.

Here, we have stopped the Taylor expansion at the term in $f(n)^2$. This means that the approximation is in $O\left(\frac{f(n)^3}{\sqrt{n}}\right)$. So it is $o(1)$ only if $f = o\left(n^{\frac{1}{6}}\right)$.

If f were to be at least in $O\left(n^{\frac{1}{6}}\right)$, the approximation would be in $O\left(\frac{f(n)^3}{\sqrt{n}}\right)$ instead of $o(1)$, so some columns of Table 5 would no longer be significant, as η . Column ϵ is no longer significant if f is at least in $O(n^{\frac{1}{6}} \ln(n)^{\frac{1}{3}})$.

Conversely, for columns γ , δ and ζ of Table 5 to be significant (i.e. not in $o(1)$), f should not be too small. Indeed, information in $o(1)$ is useless. In fact, γ is significant only if f is at least in $O\left(\frac{1}{\sqrt{n}\ln(n)}\right)$. Similarly for δ is significant only if f is at least in $O\left(\frac{1}{\sqrt{n}}\right)$ and ζ is significant only if f is at least in $O(1)$.

$\ln\Gamma(x_n) = n \ln(n) \cdot \alpha_{x_n} + n \cdot \beta_{x_n} + \sqrt{n} \ln(n) f(n) \cdot \gamma_{x_n} + \sqrt{n} f(n) \cdot \delta_{x_n} + \ln(n) \cdot \epsilon_{x_n} + f(n)^2 \cdot \zeta_{x_n} + \eta_{x_n} + o(1)$	α_{x_n}	β_{x_n}	γ_{x_n}	δ_{x_n}	ϵ_{x_n}	ζ_{x_n}	η_{x_n}
x_n with $n_2 = \frac{n+1}{2}$	α_{x_n}	β_{x_n}	γ_{x_n}	δ_{x_n}	ϵ_{x_n}	ζ_{x_n}	η_{x_n}
$\frac{n+1}{2} - \sqrt{n_2}f(n)$	$\frac{1}{2}$	$-\frac{1}{2}(1 + \ln(2))$	$-\frac{1}{\sqrt{2}}$	$\frac{1}{\sqrt{2}}\ln(2)$	0	$\frac{1}{2}$	$\frac{1}{2}\ln(2\pi)$
$\frac{n+3}{2} + \sqrt{n_2}f(n)$	$\frac{1}{2}$	$-\frac{1}{2}(1 + \ln(2))$	$\frac{1}{\sqrt{2}}$	$-\frac{1}{\sqrt{2}}\ln(2)$	1	$\frac{1}{2}$	$\frac{1}{2}\ln\left(\frac{\pi}{2}\right)$
$\frac{3n+3}{2} - \sqrt{n_2}f(n)$	$\frac{3}{2}$	$-\frac{3}{2}\left(1 - \ln\left(\frac{3}{2}\right)\right)$	$-\frac{1}{\sqrt{2}}$	$-\frac{1}{\sqrt{2}}\ln\left(\frac{3}{2}\right)$	1	$\frac{1}{6}$	$\frac{1}{2}\ln\left(\frac{9\pi}{2}\right)$
$\frac{3n+1}{2} + \sqrt{n_2}f(n)$	$\frac{3}{2}$	$-\frac{3}{2}\left(1 - \ln\left(\frac{3}{2}\right)\right)$	$\frac{1}{\sqrt{2}}$	$\frac{1}{\sqrt{2}}\ln\left(\frac{3}{2}\right)$	0	$\frac{1}{6}$	$\frac{1}{2}\ln(2\pi)$

Table 5: Approximations of $\ln\Gamma(x)$ for different reals x (in ascending order), using Stirling's formula: $\ln\Gamma(x_n) = \alpha_{x_n}n \ln(n) + \beta_{x_n}n + \gamma_{x_n}\sqrt{n}\ln(n)f(n) + \delta_{x_n}\sqrt{n}f(n) + \epsilon_{x_n}\ln(n) + \zeta_{x_n}f(n)^2 + \eta_{x_n} + o(1)$, f being positive and such that $f = o\left(n^{\frac{1}{6}}\right)$.

Final results for the approximation of the value in B_l

The previous paragraph leads to the following approximation, when $k = l = n_2$ and $r = \frac{n-1}{2} - \sqrt{\frac{n+1}{2}}f(n)$, with $f = o\left(n^{\frac{1}{6}}\right)$ (B_l):

$$\ln\Gamma(k+l+r+1) + \ln\Gamma(3n-k-l-r+1) - \ln\Gamma(r+1) - \ln\Gamma(n-r+1) = 2n\ln(n) - (2(1+\ln(2)) - 3\ln(3))n - \frac{2}{3}f(n)^2 + \ln(3) + o(1).$$

Summing all parts for the approximation of $\ln(B^{k,l,r})$ value in B_I , leads to:

$$\ln(B^{n_2, n_2, \frac{n-1}{2} - \sqrt{n}f(n)}) = -2\ln(n) - \frac{2}{3}f(n)^2 - \ln\left(\frac{\pi}{6}\right) + o(1).$$

Finally, in B_I , $B^{n_2, n_2, \frac{n-1}{2} - \sqrt{n}f(n)}$ reads:

$$B^{n_2, n_2, \frac{n-1}{2} - \sqrt{n}f(n)} \sim \frac{2}{n^2 e^{\frac{2}{3}f(n)^2} \pi \sqrt{3}} = O\left(n^{-2} e^{-\frac{2}{3}f(n)^2}\right). \quad (30)$$

C Vote correlation differences between IC , IAC^* and IAC

The purpose of this appendix is purely illustrative. It aims to describe through their induced individual votes correlation matrices the differences between the three probabilistic models described in this paper, namely IC , IAC^* and IAC . The illustration is provided for the case of three districts and three voters per district but it remains valid for any number of districts and any number of voters per district.

The matrix of correlation attached to IC is:

$$\begin{pmatrix} 1 & 0 & 0 & 0 & 0 & 0 & 0 & 0 & 0 \\ 0 & 1 & 0 & 0 & 0 & 0 & 0 & 0 & 0 \\ 0 & 0 & 1 & 0 & 0 & 0 & 0 & 0 & 0 \\ 0 & 0 & 0 & 1 & 0 & 0 & 0 & 0 & 0 \\ 0 & 0 & 0 & 0 & 1 & 0 & 0 & 0 & 0 \\ 0 & 0 & 0 & 0 & 0 & 1 & 0 & 0 & 0 \\ 0 & 0 & 0 & 0 & 0 & 0 & 1 & 0 & 0 \\ 0 & 0 & 0 & 0 & 0 & 0 & 0 & 1 & 0 \\ 0 & 0 & 0 & 0 & 0 & 0 & 0 & 0 & 1 \end{pmatrix}$$

The three diagonal blocks are the 3×3 identity matrix while the six 3×3 off-diagonal blocks have only 0 entries. The IC model implies that there is no correlation among individual votes within and across districts.

In contrast, the matrix of correlation attached to IAC^* is:

$$\begin{pmatrix} 1 & \frac{1}{3} & \frac{1}{3} & 0 & 0 & 0 & 0 & 0 & 0 \\ \frac{1}{3} & 1 & \frac{1}{3} & 0 & 0 & 0 & 0 & 0 & 0 \\ \frac{1}{3} & \frac{1}{3} & 1 & 0 & 0 & 0 & 0 & 0 & 0 \\ 0 & 0 & 0 & 1 & \frac{1}{3} & \frac{1}{3} & 0 & 0 & 0 \\ 0 & 0 & 0 & \frac{1}{3} & 1 & \frac{1}{3} & 0 & 0 & 0 \\ 0 & 0 & 0 & \frac{1}{3} & \frac{1}{3} & 1 & 0 & 0 & 0 \\ 0 & 0 & 0 & 0 & 0 & 0 & 1 & \frac{1}{3} & \frac{1}{3} \\ 0 & 0 & 0 & 0 & 0 & 0 & \frac{1}{3} & 1 & \frac{1}{3} \\ 0 & 0 & 0 & 0 & 0 & 0 & \frac{1}{3} & \frac{1}{3} & 1 \end{pmatrix}$$

The three diagonal blocks are now the 3×3 matrix $\begin{pmatrix} 1 & \frac{1}{3} & \frac{1}{3} \\ \frac{1}{3} & 1 & \frac{1}{3} \\ \frac{1}{3} & \frac{1}{3} & 1 \end{pmatrix}$ while the six 3×3 off-diagonal blocks continue to have only 0 entries. The IAC^* model implies, like the IC model, that there is no correlation among individual votes across districts but in contrast to the IC model, we have now a correlation of $\frac{1}{3}$ between the votes of two voters belonging to the same district. There is a probability of $\frac{2}{3}$ that any two voters from the same district share the same preference and a probability of $\frac{1}{2}$ that any two voters from different districts share the same preference.

Finally, the matrix of correlation attached to IAC is:

$$\begin{pmatrix} 1 & \frac{1}{3} & \frac{1}{3} & \frac{1}{3} & \frac{1}{3} & \frac{1}{3} & \frac{1}{3} & \frac{1}{3} & \frac{1}{3} \\ \frac{1}{3} & 1 & \frac{1}{3} & \frac{1}{3} & \frac{1}{3} & \frac{1}{3} & \frac{1}{3} & \frac{1}{3} & \frac{1}{3} \\ \frac{1}{3} & \frac{1}{3} & 1 & \frac{1}{3} & \frac{1}{3} & \frac{1}{3} & \frac{1}{3} & \frac{1}{3} & \frac{1}{3} \\ \frac{1}{3} & \frac{1}{3} & \frac{1}{3} & 1 & \frac{1}{3} & \frac{1}{3} & \frac{1}{3} & \frac{1}{3} & \frac{1}{3} \\ \frac{1}{3} & \frac{1}{3} & \frac{1}{3} & \frac{1}{3} & 1 & \frac{1}{3} & \frac{1}{3} & \frac{1}{3} & \frac{1}{3} \\ \frac{1}{3} & \frac{1}{3} & \frac{1}{3} & \frac{1}{3} & \frac{1}{3} & 1 & \frac{1}{3} & \frac{1}{3} & \frac{1}{3} \\ \frac{1}{3} & \frac{1}{3} & \frac{1}{3} & \frac{1}{3} & \frac{1}{3} & \frac{1}{3} & 1 & \frac{1}{3} & \frac{1}{3} \\ \frac{1}{3} & \frac{1}{3} & \frac{1}{3} & \frac{1}{3} & \frac{1}{3} & \frac{1}{3} & \frac{1}{3} & 1 & \frac{1}{3} \\ \frac{1}{3} & \frac{1}{3} & \frac{1}{3} & \frac{1}{3} & \frac{1}{3} & \frac{1}{3} & \frac{1}{3} & \frac{1}{3} & 1 \end{pmatrix}$$

The three diagonal blocks continue to be the 3×3 matrix $\begin{pmatrix} 1 & \frac{1}{3} & \frac{1}{3} \\ \frac{1}{3} & 1 & \frac{1}{3} \\ \frac{1}{3} & \frac{1}{3} & 1 \end{pmatrix}$ while the six 3×3 off-diagonal blocks are now the 3×3 matrix $\begin{pmatrix} \frac{1}{3} & \frac{1}{3} & \frac{1}{3} \\ \frac{1}{3} & \frac{1}{3} & \frac{1}{3} \\ \frac{1}{3} & \frac{1}{3} & \frac{1}{3} \end{pmatrix}$. The IAC model implies that there is a correlation of $\frac{1}{3}$ between the votes of any two voters irrespective of their district affiliation. There is a probability of $\frac{2}{3}$ that any two voters share the same preference. Among the features of the IAC model that deserve to be emphasized, we would like to call the attention on uniformity : the correlation is equal to $\frac{1}{3}$ for any pair of voters which is considered while in the IAC^* model it holds true only for voters from the same district. This observation suggests an immediate gen-

eralization of the *IC*, *IAC** and *IAC* models. Just consider a 9×9 matrix where the three diagonal blocks would be $\begin{pmatrix} 1 & \rho^{intra} & \rho^{intra} \\ \rho^{intra} & 1 & \rho^{intra} \\ \rho^{intra} & \rho^{intra} & 1 \end{pmatrix}$ where $\rho^{intra} \in [0, 1]$ denotes the correlation between the votes of any two voters from the same district and where the six off-diagonal blocks would be $\begin{pmatrix} \rho^{inter} & \rho^{inter} & \rho^{inter} \\ \rho^{inter} & \rho^{inter} & \rho^{inter} \\ \rho^{inter} & \rho^{inter} & \rho^{inter} \end{pmatrix}$ where $\rho^{inter} \in [0, 1]$ denotes the correlation between the votes of any two voters from different districts. This probabilistic model remains very special as it is very symmetric and defined exclusively by two parameters. But it contains the three popular models as special cases. We have respectively : $\rho_{IC}^{intra} = \rho_{IC}^{inter} = 0$, $\rho_{IAC^*}^{intra} = \frac{1}{3}$ and $\rho_{IAC^*}^{inter} = 0$ and $\rho_{IAC}^{intra} = \rho_{IAC}^{inter} = \frac{1}{3}$.

The main message of this paper is that the *IAC* probability of an election inversion converges to 0 at a speed equal to $\frac{1}{\sqrt{n}}$ where n denotes the number of voters in a district. The rarity of the paradox arises from the fact that under *IAC*, the electorate is likely to be very homogeneous since $\frac{1}{3}$ is already a significant value. In the limit, when $\rho^{intra} = \rho^{inter} = 1$ i.e. when the society is populated by clones, the paradox vanishes completely. On the other hand, if a significant correlation exists but is limited to voters from the same district, the paradox does not disappear in the limit as the probability is 12.5%. The lesson that can be drawn from that is that we can likely generate all sorts of patterns by considering various values of ρ^{intra} and ρ^{inter} .

For the sake of illustration, consider the following simple²³ generalization of *IAC*. Instead of drawing the Bernoulli parameter p uniformly in $[0, 1]$, we draw p uniformly in the interval $[\frac{1}{2} - \delta, \frac{1}{2} + \delta]$ where δ is a parameter in $[0, \frac{1}{2}]$. *IAC** is not covered by this model but *IC* and *IAC* are : *IC* corresponds²⁴ to $\delta = 0$ while *IAC* corresponds to $\delta = \frac{1}{2}$. The probability that any two voters vote democrat is:

$$\frac{1}{2\delta} \int_{\frac{1}{2}-\delta}^{\frac{1}{2}+\delta} p^2 dp = \frac{1}{4} + \frac{\delta^2}{3}$$

Therefore:

$$\rho_{\delta} \equiv \rho^{intra} = \rho^{inter} = \frac{4\delta^2}{3}$$

Unsurprisingly, when δ tends to 0, ρ_{δ} tends to 0 while when δ tends to $\frac{1}{2}$, ρ_{δ} tends to $\frac{1}{3}$. We could revisit the evaluation of the probability of election inversions done in that paper for this general model for an arbitrary value of δ and thus an arbitrary value of ρ .

To do so we have cooked up a computer program that simulate the electoral outcomes of the electoral college for any number of districts for any large number of voters up to 10^8 voters per district

²³Other ways to generate correlation among Bernoulli variables exist. For instance, we could use a beta distribution instead of this truncated uniform distribution or the Gaussian distribution as in Le Breton, Lepelley and Smaoui (2016).

²⁴Strictly speaking the density is not defined for $\delta = 0$. *IC* is truly the limit when $\delta \rightarrow 0$.

and for any value of the parameter δ . The simulations confirm that when δ tends to 0 the probability of election inversions tends to 20% while it tends rapidly to 0 for large values of n when δ tends to $\frac{1}{2}$. For realistic values of n say²⁵ n around 10^6 and say 51 districts instead of 3, the probability of election inversions is equal to 4% (the empirical frequency of the paradox in U.S. presidential elections) when $\delta = 0.00037$ i.e. $\rho = 1.8 \times 10^{-7}$. So a very small amount of correlation (but certainly not $\frac{1}{3}$) is enough to generate a small, but not degenerate, frequency of the election inversion paradox for large populations of voters²⁶.

D Functions coded in C

The library of files `codeC.dll` contains the following functions which will be run in C from R:

- `loggamma3`: allows to obtain a table containing the values of the function $\ln \Gamma$ (computed using Stirling's formula),
- `IAC`: computation of $\tilde{\phi}$ (for as much values of n as necessary),
- `IAC_maj`: computation of $\tilde{\phi}_{maj}$ (for as much values of n as necessary),
- `IAC_min`: computation of $\tilde{\phi}_{min}$ (for as much values of n as necessary),
- `IAC_par`: parallel computation of $\tilde{\phi}$ (for a unique value of n).

We upload these functions from the file `codeC.dll` as follows²⁷

```
> dyn.load("code/codeC.dll")
```

D.1 Function `loggamma3`

```
void loggamma3(double *lgamm, int *taillelgamm)
```

- `lgamm`: a vector of double (initialized at 0), of dimension `taillelgamm`,
- `taillelgamm`: an integer containing the size of the table that we want to consider.

²⁵Precisely, $n = 2 \times 10^6 + 1$ and 10^6 simulations.

²⁶This exercise is theoretical and is by no means intended to suggest that this model fits the data. It simply points out the impact of the specific value of the correlation coefficient on the probability of election inversion.

²⁷To do so, we must check that the inputs are in the right format.

Illustration

We want to compute $\tilde{\phi}$ for $n \leq 1001$. To do so we need the vector $\ln \Gamma$ for the integers ranging from 1 to $3n_{max} + 2$ with $n_{max} = 1001$. We store these values in the object `lg`.

```
> n.max=1001
> lg<-C("loggamma3", lgamm=as.double(rep(0,3*n.max+2)),
+  taillelgamm=as.integer(3*n.max+2))$lgamm
```

D.2 Function *IAC*

```
void $IAC$(double *phi, double *n, int *taille, double *lgamm,
double *eps, double *nb_calc, double *approx)
```

- `phi`: a vector of `double` (initialized at 0) of dimension `taille` containing all the values of $\tilde{\phi}$,
- `n`: a vector of `double` (to be specified by the user) of dimension `taille` containing the values of n ,
- `taille`: an integer (to be specified by the user) corresponding to the number of values to be calculated,
- `lgamm`: a vector of dimension $3n_{max} + 2$ containing the values of $\ln \Gamma$, where $n_{max} = \max(n)$,
- `eps`: a `double` (to be specified by the user) corresponding to the value of ε ,
- `nb_calc`: a vector of `double` (initialized at 0) of dimension `taille` corresponding to the number of expressions which have been calculated,
- `approx`: a vector of `double` (initialized at 0) of dimension `taille` delivering $Err = Err_1 + Err_2 + Err_3$.

Illustration We want to compute $\tilde{\phi}$ for two values: $n = 101$ and $n = 1001$.

```
> n<-c(101,1001)
```

To invoke the function *IAC*, we need to specify ε :

```
> precision = 25
> eps=10^(-precision)
```

We invoke the function *IAC* as follows:

```
> res<-.C("$IAC$", phi=as.double(rep(0,2)), n=as.double(n),
+ taille=as.integer(2), lgamm=as.double(lg), eps=as.double(eps),
+ nb_calc=as.double(rep(0,2)), approx=as.double(rep(0,2)))
```

The object `res` contains the values of $\tilde{\Phi}$:

```
> print(res$phi, 20)
```

```
[1] 0.0128348271775305423914 0.0041318201550210147122
```

we can multiply these numbers by \sqrt{n} :

```
> print(sqrt(n)*res$phi, 20)
```

```
[1] 0.12898841675276404017 0.13072493920913225152
```

The object `res` contains the number of computations which have been done:

```
> res$nb_calc
```

```
[1] 6681 202011
```

It also contains the approximation errors Err resulting from the choice of ϵ :

```
> res$approx
```

```
[1] 3.825876e-21 2.470091e-19
```

D.3 Function `IAC_maj`

```
void $IAC$_maj(double *phi, double *n, int *taille, double *lgamm,
              double *eps, double *r_min, double *approx_maj)
```

- `phi`: vector of double (initialized at 0) of dimension `taille` containing the values of $\tilde{\Phi}_{maj}$,
- `n`: vector of double ((to be specified by the user) of dimension `taille` containing the values of n ,
- `taille`: an integer ((to be specified by the user) giving the number of values to be calculated,
- `lgamm`: a vector of dimension $3n_{max} + 2$ containing the values of $\ln \Gamma$, where $n_{max} = \max(n)$,
- `eps`: a double ((to be specified by the user) specifying the value of ϵ ,
- `r_min`: a vector of double (initialized at 0) of dimension `taille` delivering the values r_{min} ,
- `approx_maj`: a vector of double (initialized at 0) of dimension `taille` giving Err_1 .

Illustration

We want to compute $\tilde{\Phi}_{maj}$ for the same values of n and ε :

```
> majorant<-.C("$IAC$_maj", phi=as.double(rep(0,2)), n=as.double(n),
+ taille=as.integer(2), lgamm=as.double(lg), eps=as.double(eps),
+ r_min=as.double(rep(0,2)), erreur1=as.double(rep(0,2)))
```

Then we depict the values of $\tilde{\Phi}_{maj}$, $\sqrt{n} \times \tilde{\Phi}_{maj}$, the approximation errors Err_1 and the values r_{min} which will be stored in the object `r_min` for subsequent use:

```
> print(majorant$phi, 20)
```

```
[1] 0.0270715553140992437609 0.0096017241779385118644
```

```
> print(sqrt(n)*majorant$phi, 20)
```

```
[1] 0.27206576377699165370 0.30378495732408838936
```

```
> majorant$erreur1
```

```
[1] 1.816305e-23 1.882691e-20
```

```
> (r_min<-majorant$r_min)
```

```
[1] 1 325
```

D.4 Function `IAC_min`

```
void $IAC$_min(double *phi, double *n, int *taille, double *lgamm,
              double *eps, double *k_max, double *r_min,
              double *erreur2, double *erreur1_prime)
```

- `phi`: vector of double (initialized at 0) of dimension `taille` containing the values of $\tilde{\Phi}_{maj}$,
- `n`: vector of double ((to be specified by the user) of dimension `taille` containing the values of n ,
- `taille`: an integer ((to be specified by the user) giving the number of values to be calculated,
- `lgamm`: a vector of dimension $3n_{max} + 2$ containing the values $\ln \Gamma$, where $n_{max} = \max(n)$,
- `eps`: a double ((to be specified by the user) specifying the value of ε ,

- `k_max`: a vector of double (initialized at 0) of dimension `taille` delivering the values k_{max} ,
- `r_min`: a vector of double ((to be specified by the user) of dimension `taille` delivering the values r_{min} ,
- `erreur2`: a vector of double (initialized at 0) of dimension `taille` delivering Err_2 ,
- `erreur1_prime`: a vector of double (initialized at 0) of dimension `taille` delivering Err'_1 .

Illustration

We want to compute $\tilde{\Phi}_{min}$ for the same values of n and ε :

```
> minorant<-.C("$IAC$_min", phi=as.double(rep(0,2)), n=as.double(n),
+ taille=as.integer(2), lgamm=as.double(lg), eps=as.double(eps),
+ k_max=as.double(rep(0,2)), r_min=as.double(r_min),
+ erreur2=as.double(rep(0,2)), erreur1_prime=as.double(rep(0,2)))
```

OWe depict the values of $\tilde{\Phi}_{min}$, $\sqrt{n} \times \tilde{\Phi}_{min}$, Err'_1 and Err_2 . We store the values k_{max} for subsequent use

```
> print(minorant$phi, 20)
```

```
[1] 0.0073237458834344215317 0.0020649699772476888537
```

```
> print(sqrt(n)*minorant$phi, 20)
```

```
[1] 0.073602735209212066803 0.065332726163395749008
```

```
> minorant$erreur1_prime
```

```
[1] 4.190794e-23 2.737040e-21
```

```
> minorant$erreur2
```

```
[1] 1.132576e-25 1.240105e-23
```

```
> (k_max<-minorant$k_max)
```

```
[1] 83 603
```

D.5 Function `IAC_par`

```
void $IAC$_par(double *phi, double *n, double *lgamm, double *eps,
              int *r_min, int *k_max, double *x, double *nbcpus,
              double *approx)
```

- `phi`: one value of `double` (initialized at 0) containing the value of $\tilde{\phi}$ calculated for the set of values $\{k_i\}$ defined for $i = 1, \dots, \text{npcpus}$ and such that $\{k_i = (k_{max} + 1 - i) - \text{npcpus} \times j \geq \frac{n+1}{2}, \text{ with } j = 1, 2, \dots\}$, and where `n`, `k_max` and `nbcpus` are specified by the users,
- `n`: One value of `double` (to be defined by the user) containing the value of n ,
- `lgamm`: vector of dimension $3n + 2$ containing the values of $\ln \Gamma$,
- `eps`: one `double` ((to be specified by the user) specifying the value of ε ,
- `r_min`: a `double` ((to be specified by the user and obtained from the function `IAC_maj`) delivering the value of r_{min} ,
- `k_max`: a `double` ((to be specified by the user and obtained from the function `IAC_min`) delivering the value of k_{max} ,
- `x`: a `double` ((to be specified by the user) which changes depending upon the core on which the calculation is sent. $x = (k_{max} + 1 - i)$ with $i = 1, \dots, \text{npcpus}$,
- `nbcpus`: a `double` ((to be specified by the user) giving the number of cores where is sent the computation of $\tilde{\phi}$,
- `approx`: a `double` (initialized at 0) delivering Err_3 .

Illustration To run parallel computing, we have to create a function which allows to send on `IAC_on` several cores via a simple modification of the parameter `x`. This function is called `calpar1`.

```
> calpar1<-function(x, n, r_min, k_max, lgamm, eps, nbcpus)
+ { + dyn.load("C:/Users/laurent/Desktop/michel
lebreton/code/codeC.dll") + res2<-.C("$IAC$_par", phi=as.double(0),
n=as.double(n), + lgamm=as.double(lgamm), eps= as.double(eps),
r_min=as.integer(r_min), + k_max=as.integer(k_max),
x=as.double(x), nbcpus=as.double(nbcpus), +
approx=as.double(rep(0,2))) +
return(list(phi=res2$phi,nb_calc=res2$approx[2],approx3=res2$approx[1]))
+ }
```

We will compute $\tilde{\phi}$ for $n = 1001$ on 4 processors:

```
> nbcpus=4
```

The values of x to be initialized are:

```
> (x=(k_max[2]+1)-0:(nbcpus-1))
```

```
[1] 604 603 602 601
```

To run the parallel computing:

```
> require("snowfall")
```

```
> sfInit(parallel=TRUE, cpus=nbcpus)
```

```
R Version: R Under development (unstable) (2014-06-11 r65921)
```

```
> result2 <-sfClusterApplyLB(x, calpar1, 1001, r_min[2], k_max[2],  
+ lg, eps, nbcpus)
```

```
> sfStop()
```

The returned object contains the peices of $\tilde{\phi}$:

```
> unlist(lapply(result2, function(x) x$phi))
```

```
[1] 0.0006837732 0.0008864855 0.0011330502 0.0014285113
```

We then aggregate the values of $\tilde{\phi}$ and the number of calculations:

```
> print(sum(unlist(lapply(result2, function(x) x$phi))), 20)
```

```
[1] 0.0041318201550210138448
```

```
> print(sum(unlist(lapply(result2, function(x) x$nb_calc))), 20)
```

```
[1] 202011.0000000000000000
```

To recover the approximation error, we sum the approximation errors Err_1, Err_2, Err_3 :²⁸

```
> majorant$erreur1[2] + minorant$erreur2[2] +
```

```
+ sum(unlist(lapply(result2, function(x) x$approx3)))
```

```
[1] 2.470091e-19
```

²⁸Until the 17th decimal, we get the same values as those obtained without parallel computing. The differences which appear then result from the fact that the sum of the expressions $B^{k,l,r}$ does not follow the same order n the case of parallel computing.